中國山水畫山石皴法合成技術之研究

研究生: 魏德樂　　　　　　　　　　　指導教授: 施仁忠 教授

國立交通大學　　資訊學院　　資訊工程學系

摘　　要

　　電腦圖學自三十多年以來，追求逼真一直是不變的目標。所以各專家學者不斷研究新的方法，以更接近真實與具物理特性的運作環境。而追求逼真的目標之餘，有些效果卻是連真實世界都無法呈現的。藝術化視覺資訊在日常生活中也佔極重要的地位，它與視覺資訊同為人類感官功能中所最常接觸的資料型態，而藝術化視覺資訊更能引發人類的內心的感覺。當真實視覺資訊技術已逐漸成熟之時，近年來已有許多科學家研究印象派畫家電腦自動產生技術，此即是電腦圖學的一分支領域所專注之處，有別於前者，此領域名稱取為 NPR(Non-Photorealistic Rendering)。NPR 的目標其中包括了模擬人類各種繪畫風格，每年電腦圖學相關的國際研討會討論此領域技術之計劃也逐年以驚人的速度激增，顯示此領域技術逐漸受人重視。

　　中國國畫具有悠久的歷史，我國傳統繪畫藝術之一，在世界美術領域中自成體系。而山水畫於東晉時期萌芽，經一千六百多年眾名家不斷傳承創新下，累積了無數的技術經驗。由於它的技法複雜、山川變化大、題材多，光是運筆用墨上，便需很多時間磨練。在中國山水畫中，山石場景為首要的描寫對象之一，峯巒山石聯綴而成的優美律動，構成生靈活潑、含蘊無窮之山水畫境。目前有許多 NPR 的研究論文都著重在西畫的模擬，

譬如鉛筆、油畫或水彩等，這些研究已經為西部繪畫模擬出好結果。但這些方法不適合中國水墨畫，通常西方繪畫需要更多的精確度，但中國墨水繪畫是比較抽象的。另外，筆墨的模擬在中國水墨畫是主要的工作，包括水墨擴散，乾溼筆的順序和各種各樣的筆觸大小和技術細節等，和西方繪畫的屬性完全不同。

在本論文中，我們提出「中國山水畫山石皴法合成技術之研究」。主要貢獻如下：完成毛筆的模型，並控制墨的「水分」，讓其自然滲化、溶接，產生不同的墨色效果。自動產生皴法的紋理，使用控制線及起始位置與結束位置，依山石的紋理以各種線條，畫出石頭的質感或立體感。首先，我們將定義基本皴法的參數，包括用墨濃淡，墨的水分多少，以及交錯的形式與方向等等。這些基本參數構成我們皴法筆觸的原型。我們可以事先透過不同的參數組合，先完成一部份的皴法筆觸。我們得到向量化的資料之後，就可以為皴法筆觸定義出起點以及終點。定義的方式當然可以自動，或是透過使用者完成。有了筆觸的起點以及終點之後，自然筆劃的方向就大致確定。最後，起始點用淡墨，終點用濃墨，再自動皴法筆觸，加以適合地動態調整，而形成我們所需要的一筆皴法。同樣的原理將重複運用，直到整個水墨畫完成為止。這一套自動化的描繪過程首先擷取三維山石模型的幾何形狀資訊，建立各類資訊的索引圖，從中分析以獲致描繪形狀與表皮紋理（皴法）的參考依據，然後產生適當的勾勒筆觸，及變化豐富的皴擦渲染效果，自動畫出俱山水畫風格的山川石岩，而成一幅幅引人入勝的山水畫作與具有中國水墨畫風格的 3D 動畫。

The Synthesis of Rock Textures

in Chinese Landscape Painting

Student: Der-Lor Way   Advisor: Dr. Zen-Chung Shih

Department of Computer Science and Information Engineering

College of Computer Science

National Chiao-Tung University

ABSTRACT

Computer graphics-related research has focused on obtaining photorealistic images. However, photorealism is occasionally not the most effective means of visually expressing emotions. Accordingly, photographs can never entirely replace paintings. Non-photorealistic rendering (NPR) approaches have recently received renewed interest. Researchers have begun to study how a photograph or a photorealistic image may be made to look like a painting. In recently years, most research in NPR focused on Western painting. Lots of paintings algorithms have been proposed for convert a photorealistic image into an art form such as an oil painting or watercolor. Typically, such a painting style is created by applying masks or by placing user-defined patterns. These methods deliver good results for Western painting. But these approaches are not appropriate to Chinese ink painting. Generally, Western painting involves more precision but Chinese ink painting is more abstract. However, strokes in Chinese ink painting are in many aspects based on Chinese brushwork, including ink diffusion, pattern placing and describing details with various brush sizes and techniques.

Chinese ink painting stresses the notion of "implicit meaning" in which painters use a minimum amount of strokes to express their deepest feelings. Landscapes are one of the most important themes in Chinese painting. In the Tang dynasty, the range of subjects in painting expanded and landscape became established as a distinct category. Chinese landscape painting provided a more spontaneous style that captured images in abbreviated suggestive forms. Chinese landscape painting has been cultivated by masters through a long evolution into an exquisite art form.

To simulate the style of Chinese landscape painting is not trivial at all. It usually uses brushes and ink as mediums, values the expression of the artistic conception far beyond the precise appearance of the painted subjects. By means of the blending effects of brushes and ink, painters communicate their frame of mind to the viewers. This thesis proposes a set of methods to automatically create 3D animation of Chinese landscape painting. Rocks are the major painting objects in Chinese landscape painting. The given 3D models are drawn by outline rendering and texture generation, from information of the shape, shade and orientation of model's surface. Many reference maps are constructed to analyze the information; create brush strokes for the outline and texture strokes. Finally, the target of the project will automatically create the still images and animations.

The main contribution of this investigation is the modeling and implementation of six major texture strokes for terrain surface using traditional brush techniques in Chinese landscape painting. The proposed rendering technique involves many fundamental parts. First, 3D terrain information is extracted to detect the edges of the silhouettes, and to generate streamlines and ridge meshes. The outline of a silhouette is then constructed and the streamlines of the texture strokes are generated. All control lines that involve the silhouette and streamlines then are projected onto a 2D viewing plane. Brush strokes then are applied to create an outline drawing and the texture of rock is captured using vertical or slanted strokes along the control lines with a rich ink tone specified by a luminance map. Finally, the ink diffusion on the rice paper is simulated.

Acknowledgements

First of all, I would like to show my gratitude to my advisor, Prof. Zen-Chung Shih for his patience and guidance. Also, I am grateful to all the members in Computer Graphics and Virtual Reality Laboratory for their useful suggestion and encouragement in these days.

It is hard to describe that my feeling is. I shuttle back and forth in the studies, the work and the family during these years. I would like to dedicate the achievement of this work to my wife Jean. Without her endless support, I couldn't fully focus on my study. Special thanks to my mentor Ch'iu-Hsia Chang who always directs me the life-direction and helps my families. Finally, I also thanks to my father and my children. Without their unconditional love, I won't finish it.

Contents

List of Tables

List of Figures

Chapter 1
Introduction

The realism is a major goal in computer graphics from 30 years ago. Computer graphics-related research has focused on obtaining photorealistic images. Over many years, the advocate of photorealism has conceived many methods and algorithms for synthetic image generation; the dominant form is based on the physical technology. These are discovered by physical world observation driving, in the light interaction by the surface and the object in the environment. The ray tracing and the radiosity are two powerful technologies in the photorealistic rendering. In both cases, the physical behavior of light is imitated to produce the best photorealism example in a hypothesized world.

Today, it is easy and powerful to construct a photo-realistic virtual world through many developed methods and graphic accelerator. However, photorealism is occasionally not the most effective means of visually expressing emotions. Accordingly, photographs can never entirely replace paintings. Non-photorealistic rendering (NPR) approaches have recently received renewed interest. Researchers have begun to study how a photograph or a photorealistic image may be made to look like a painting. In recently years, most research in NPR focused on Western painting. Many researches have addressed Western painting, including watercolors, impressionistic painting, pencil sketches and hatching strokes. Lots of

painting-algorithms have been proposed for convert a photorealistic image into an art form such as an oil painting or watercolor. Recent research on non-photorealistic rendering has focused on modeling traditional artistic media and styles including pen-and-ink illustration and watercolor painting…etc. These methods deliver good results for Western painting. But these approaches are not appropriate to Chinese ink painting (水墨畫). Generally, Western painting involves more precision but Chinese ink painting is more abstract. To simulate the style of Chinese ink painting is not trivial at all. It usually uses brushes and ink as mediums, values the expression of the artistic conception far beyond the precise appearance of the painted subjects. By means of the blending effects of brushes and ink, a painter communicates their frame of mind to the viewers.

Chinese ink painting stresses the notion of "implicit meaning" in which painters use a minimum amount of strokes to express their deepest feelings. Landscapes are one of the most important themes in Chinese painting. In the Tang dynasty (唐朝), the range of subjects in painting expanded and landscape became established as a distinct category. Chinese landscape painting (山水畫) provided a more spontaneous style that captured images in abbreviated suggestive forms. Chinese landscape painting has been cultivated by masters through a long evolution into an exquisite art form.

1.1 Non-Photorealistic Rendering

A few years ago, non-photorealistic rendering (NPR) began to keep a technical meeting to devote the artistic expression to supply the choice the form at the SIGGRAPH conference. This research frequently is the contrast to the photorealistic rendering. The term has become adopted by the computer graphics community to denote forms of rendering that are not inherently photorealistic. The terms expressive, artistic, painterly and interpretative rendering are often preferred by researchers of the field since they convey much more definitively what is being sought. The artistry, the fine arts and explanation rendering by the domain researcher frequently likes because they explicitly convey any to seek. The NPR early researcher concentrates their attention to imitate – the tradition artistic form reproduction to the natural medium, for example pen and ink, water color and oil on canvas. The natural medium imitation could be possibly considered a branch of NPR studies. But NPR provided a wider scope and the opportunity experiment for new artistic form, or because this artistic form could be the impractical creation uses the hand.

In contrast to photorealism, in which the driving force is the modeling of physical processes and behavior of light, the processes of human perception can drive NPR techniques. This can be just as demanding as physical simulation but for different reasons – a technologist may find comfort in developing algorithms to reproduce a certain physical phenomenon that is objective and relatively predictable. Developing techniques to replace, augment or even assist the subjective processes of an artist requires a shared understanding of the use to which these techniques will be put. The finest examples of NPR work will be produced when artists and technologists work together to identify a problem and develop solutions that are

sympathetic to the creative processes. Table 1.1 provides a comparison of the trends of photorealism and NPR [53].

Table 1.1: Comparing and Contrasting Photorealism and NPR

	Photorealism	NPR
Approach	Simulation	Stylization
Characteristic	Objective	Subjective
Influences	Simulation of physical processes.	Sympathies with artistic processes; perceptual-based
Accuracy	Precise	Approximate
Deceptiveness	Can be deceptive or regarded as 'dishonest'; viewers may be misled into believing that an image is 'real'.	Honest – the observer sees an image as a depiction of a scene.
Level of detail	Hard to avoid extraneous detail; too much information; constant level of detail.	Can adapt level of detail across an image to focus the viewer's attention.
Completeness	Complete	Incomplete
Good for representing	Rigid surfaces	Natural and organic phenomena

The NPR research was possibly considered early 2D interactive paint system. Researchers have developed these technologies including 2D brush-oriented painting involving more sophisticated models for brush, canvas, strokes, etc. Many researchers have developed renderings technology that can be applied to photographic images to synthesize painterly images. One of the key approaches that separate branches of research in the field is the degree to which user intervention is required. Some researchers have favored automatic techniques that require no or very limited user input, while others use the computer to place

strokes at the guidance of the artist. 2½D paint systems have been developed in which augmented image data is used to automate paint actions initiated by the artist on pre-rendered scenes.

A more recent trend of NPR research has been the adoption of 3D techniques. The classic 3D computer graphics rendering pipeline exposes a number of opportunities within which NPR techniques can be applied to manipulate data in both 3D and 2D forms. A number of researchers have focused on providing real time algorithms for NPR which affords stylized visualizations of 3D data that can be manipulated interactively. The view-independence of some of these approaches provides obvious benefits for the generation of animation sequences.

During recent years, much research has addressed Western painting on Non-Photorealistic Rendering (NPR), including watercolors [3,11], impressionistic painting [16, 23], pencil sketches [37, 38] and hatching strokes [7,12,17,29,35,48]. These approaches deliver good results in western painting. However, these methods are inappropriate for Chinese ink painting. Chinese ink paintings typically comprise a few simple strokes intended to convey the artist's deep feelings regarding the painted object. Simulating the style of Chinese landscape painting is challenging. The style includes free brush strokes, surface wrinkle and ink diffusion (水墨渲染) on the paper [1, 8, 24].

One skill used in Western painting is using hatching strokes simultaneously to convey the type of material, tone, and form [7, 12, 17, 29, 35, 48]. Hatching describes groups of strokes with a spatially coherent direction and quality. Stroke density controls the tone of the shading, while the character and arrangement of the strokes suggests a surface texture. In pen-and-ink illustrations, variable-density hatching and complex hatch patterns convey shape,

texture and lighting. Texture strokes called "*Ts'un*" (皴法) in Chinese. However, the represented material differs from that represented by hatching. Texture strokes can be used to represent a rough, cracked surface. *Ts'un* in Chinese landscape painting is woven strokes that depict terrain textures. The main goal of this work is to develop a set of novel methods for rendering terrain wrinkles (texture strokes) in Chinese landscape painting. A specific 3D terrain model is drawn in outline (輪廓) and with texture strokes based on information on the shape, shade and orientation of the model surface.

1.2   Overview of Wrinkle Rendering Diagram

Landscapes have been the main theme of Chinese painting for over one thousand years. It is a form of non-photorealistic rendering. In Chinese landscape painting, rock textures convey the orientation of mountains and contribute to the atmosphere. Several landscape-painting skills are required to capture various types of rock. Over the centuries, masters of Chinese landscape painting have developed various texture strokes. The mature texture strokes may be divided into three groups: line, dot and plane. Chinese artists use many types of brushstrokes to depict nature. A painted of Chinese landscapes must understand both texture strokes and ink brush techniques. This thesis presents a set of novel methods for rendering rock textures in Chinese landscape painting. A 3D rock is drawn as an outline and texture strokes, using information on the shape, shade and orientation of the rock's polygonal surface. This work also uses vertical (中鋒) or slanted (側鋒) brush strokes for drawing outlines and rock textures. The main contribution of this work is on the modeling and implementation of an integrated framework for rock texture rendering using traditional brush techniques in Chinese landscape painting.

This section describes the rendering of texture strokes and the use of the traditional brush technique to create primitive strokes. Figure 1.1 illustrates the process of producing texture strokes, which includes several basic elements:

(1) 3D information extraction: 3D terrain models rendered using OpenGL include vertices, edges, faces and so on. The luminance map is specified as ink tone (墨色濃淡) values.

(2) Control line construction: a direction field on the surface is computed, silhouette lines are detected and streamlines in 3D object space are generated.

(3) Projection: all control lines, silhouette lines and streamlines are projected onto a 2D viewing plane.

(4) Brush stroke: brush strokes are applied as outlines in the drawing, and the texture strokes are vertical or slanted strokes [45] following streamlines using a rich ink tone specified by a luminance map.

(5) Ink Diffusion: the motion of ink on rice paper (宣紙) is simulated [14].

Each part of the rendering diagram, shown in Figure 1.1, builds upon the others and is crucial for developing texture stroke rendering methods. This work focuses on simulating the six main texture strokes and builds upon our virtual brush with ink diffusion [14, 45, 46]. Users can easily choose a style of texture stroke and input parameters for controlling the desired effects. The proposed method then automatically completes the painting process.

The main contribution of this investigation is the modeling and implementation of six major texture strokes for terrain surface using traditional brush techniques in Chinese landscape painting. The proposed rendering technique involves many fundamental parts, illustrated in Figure 1.1. First, 3D terrain information is extracted to detect the edges of the silhouettes, and to generate streamlines and ridge meshes. The outline of a silhouette is then

constructed and the streamlines of the texture strokes are generated. All control lines that involve the silhouette and streamlines then are projected onto a 2D viewing plane. Brush strokes then are applied to create an outline drawing and the texture of rock is captured using vertical or slanted strokes along the control lines with a rich ink tone specified by a luminance map. Finally, the ink diffusion on the rice paper is simulated [14].

1.3 Organization of the Dissertation

The rest of this thesis is organized as follows. Chapter 2 reviews works related to NPR. Chapter 3 then introduces the properties of Chinese ink painting and texture strokes used in Chinese landscape painting. Subsequently, Chapter 4 describes the process of ink diffusion in detail. Next, Chapter 5 shows the virtual brush model, the technique of vertical stroke and slanted stroke. Chapter 6 then demonstrates the texture stroke synthesis from 2-dimension picture using our proposed method. Chapter 7 shows six different rendering style of wrinkle onto the surface of 3-dimension terrain. Finally, Chapter 8 describes conclusions and suggests areas for future research.

```
                    ┌──────────────────────────┐
                    │     3D Terrain Model      │
                    └────────────┬─────────────┘
                                 ↓
                    ┌──────────────────────────┐
                    │  3D Information Extraction │
                    └────────────┬─────────────┘
           Geometry
           (vertex, edge, face, curvature)
```

Silhouette Edge Detection

Streamlines Generation

Texture Strokes
1. Hemp-Fiber
2. Axe-Cut
3. Lotus-Leaf
4. Raindrop
5. Mi-Dot
6. Boneless

Projection

Brush Stroke

Luminance map
(shading, fog effect)

Ink Tone

Ink Diffusion on a rice paper

3D Object Space

2D Image Space
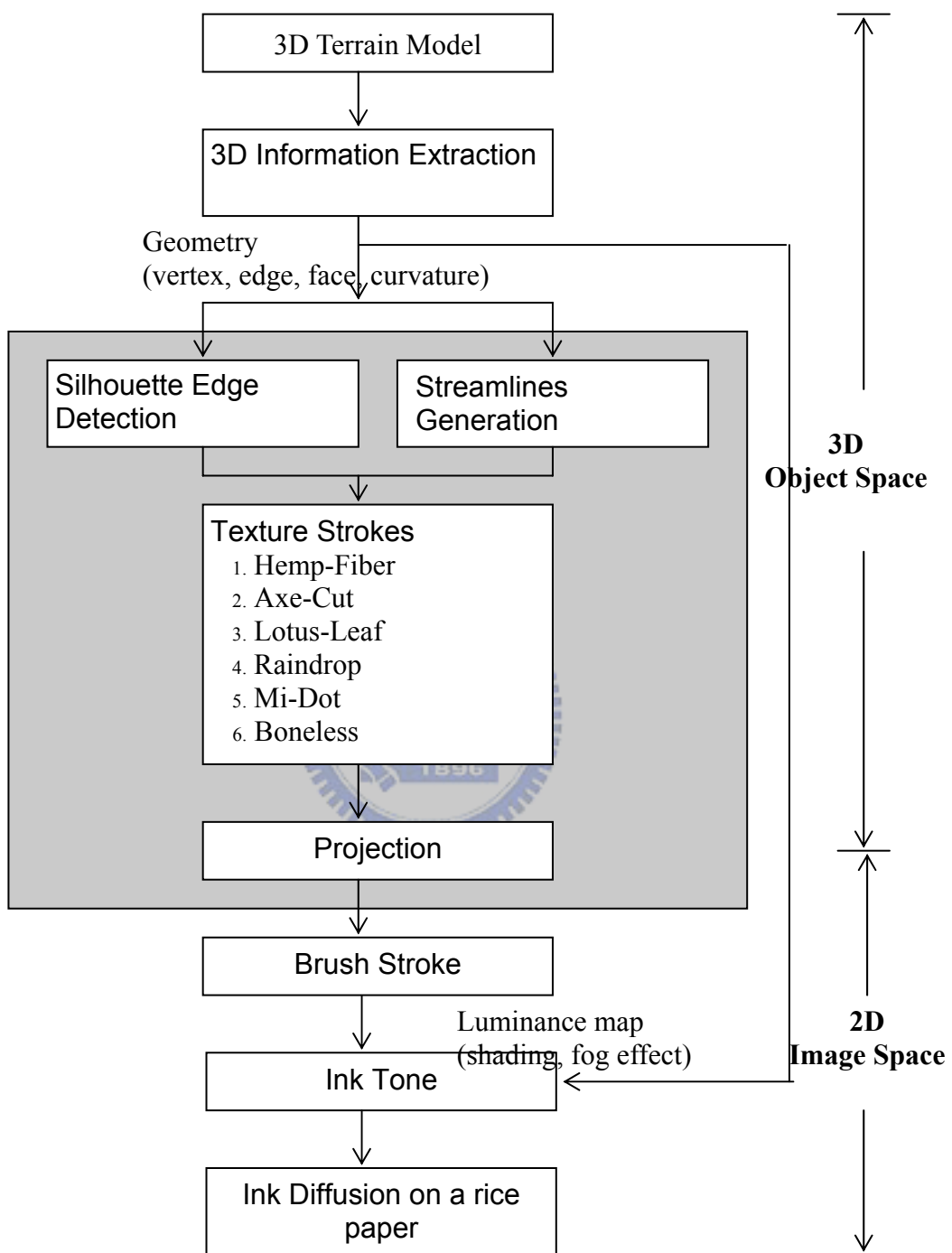
Figure 1.1 : Surface wrinkle rendering diagram.

Chapter 2
Related Works

2.1 Ink Diffusion and 2D Brush Strokes

Importantly, an artist can use thousands of styles to express his mental state while painting, using various brush storks and rich ink gradation. Ink diffusion is crucial in Chinese ink painting, and generates for example, the fluffy-edged effect, a variety of ink intensities, blurring the boundary of a stroke, the merging of two strokes, and other effects. Some particular techniques, such as, "dense brush following dilute brush" and the splashed ink painting (潑墨畫) technique are fairly important in Chinese ink painting.

Expressive brush strokes are the first requirement in Chinese landscape painting. Little research has addressed methods for simulating brush stroke and ink behavior. The brush has been simulated as a collection of bristles that evolve during a stroke. Strassmann [39] was the first to consider a hairy brush as a 1D array of bristles. Lee [19, 20] considered elastic bristles that obey Hooke's law and described diffusion rendering of black ink paintings using new paper and ink models. Guo and Kunii [9, 10] first addressed ink diffusion in 1991. The diffusion of the ink into the absorbent paper is one of the most notable features of black ink

painting (called 'Sumie' in Japanese). Zhang et al. [51] presented a 2D simple cellular automaton-based simulation of ink behavior. Furthermore, Saito and Nakajima [33] devised a 3D physics-based brush model that enables users to paint various strokes intuitively and directly on a computer with a pen-like input device. Xu et al. [49, 50] proposed a two-level hierarchical geometry model. They used three B-spline curves to control the three-dimensional brush geometry. Chu et al.[2] designed a 3D virtual brush model with ink depositing from brush to paper in real time.

Sousa and Buchanan [37, 38] focused on the technical aspects of physically simulating real media, including pencil, crayon, blenders and erasers. Watercolors have also been simulated. Small [36] proposed a parallel approach to predicting the action of the pigment and water on paper fibers. Curtis and Anderson [3] employed a more sophisticated paper model, a more complex shallow water simulation and more faithful rendering and optical composition of pigmented layers based on the Kubelka-Munk model, to simulate watercolors more realistically. Unfortunately, the properties of Chinese ink painting differ from those of watercolors. The physical behavior of watercolors differs from that of Chinese ink.

These papers proposed several methods for simulating brush strokes and the diffusion of ink. Although they realistically reproduced the diffusion of a single stroke, no mechanism has been presented to simulate the blending of two or more different kinds of brush strokes. Some results are unreasonable for Chinese ink painting. Accordingly, the simulated results in the above papers were not compared to real ink paintings.

This thesis presents a new method for simulating ink diffusion based on observation and analysis. The proposed method can simulate various expressions of tones on different types of paper. The elucidation of the effect of mixing simulated strokes made by different kinds of

brushes is an important contribution of the method. Finally, the simulated results are compared with real ink painting.

2.2   3D Non-Photorealistic Rendering

This work is also related to research on 3D non-photorealistic rendering, [4, 13, 15, 16] including stylized line illustrations, artistic hand-drawn illustrations and hatching painting styles. Many studies have addressed the problem of generating silhouettes and high-quality hatching of static scenes. Markosian et al. [25] presented a randomized algorithm for locating silhouettes. Moreover, Winkenbach and Salesin [48] designed a method of rendering smooth surfaces with pen-and-ink. Salisbury et al. [35] introduced prioritized stroke textures with tone values that are mapped to the stroke arrangements, and presented impressive examples of computer-generated hatching. Furthermore, Sousa and Buchanan [37, 38] focused on the technical aspects of physically simulating real media, including pencil, crayon, blenders and erasers. Hertzmann and Zorin [12] generated high-quality silhouettes and established a scheme for placing image-space strokes for cross-hatching. Moreover, Lake et al. [17] described an interactive hatching system with stroke coherence in the image space. Finally, the method of Freudenberg [7] involved encoding a stroke texture as a halftone pattern.

Surface rendering using principle curvature directions has recently become an extremely popular technique for non-photorealistic rendering. Elberg [6] and Interrante used principal curvature directions for hatching. Curvatures normally provide good hatch directions. The most natural geometric candidate is the pair of principal curvature direction fields [6, 41]. Rössl et al. [30, 31, 32,] provided a new approach for automatically generating a direction field for the strokes. Discrete curvature analysis of such meshes permits the estimation of

differential parameters. Curvature lines are then constructed and used as strokes. This work also designs a simple weighted technique that uses a reference direction generating smooth direction fields on a surface, which are suitable for generating streamlines for texture strokes of the surface of a terrain.

Freudenberg's method involves encoding a stroke texture as a halftone pattern. The "height" of the corresponding location in the pattern is compared to each pixel's target tone using a "soft" threshold function to shade a pixel. Emil Praun [29] described how prioritized stroke textures could be rendered efficiently using texture hardware by pre-computing a tonal art map (TAM).

In scientific and engineering applications, there is also a need to abstract other form-defining cues from a grid Digital Elevation Model (DEM). Visvalingam et al. [42, 43] showed the possibility of automatically abstracting a type of static 2.5D sketch called the profile-stroke (P-stroke) sketch. Lesage and Visvalingam [21] reviewed an image-based approach for deriving artistic sketches of terrain surfaces. Lesage and Visvalingam used a 3D visualization system for rendering luminance maps of different type of terrain, and compared four common image-based edge detectors for extracting the sketches. Although Lesage and Visvalingam reproduced pen, pencil and charcoal sketching styles that can be obtained by adjusting the grey scale and thickness of output primitives, unfortunately these styles of sketching differ from the properties of Chinese painting.

Sato et al. [34] extend their previous work to generate sumi-e like paintings of arbitrary objects from three-dimensional polygonal models. Their proposed method realizes three brush stroke (Kou, Ten, and Shun) techniques for generating landscapes paintings. A Kou stroke is generated for line drawing; a Ten stroke has the shape like a grain of rice, which is similar to

dot stroke (Fig 1(d) (e)); a Shun stroke has the shape like a *hemp-fiber* stroke (Fig 1(a), 批麻皴).

This thesis modeled the effects of brush strokes in traditional Chinese ink painting. That investigation simulated two fundamental brush strokes, namely vertical and slanted strokes. An interactive tool for painting two rock textures (*hemp-fiber* and axe-cut(斧劈皴)) on a 2D image was also presented. Furthermore, a method [14] of simulating the diffusion of ink on rice paper was provided. The proposed method was based on a physical mechanism and observational model of the interaction among real drawing materials used in Chinese ink painting and of the variation in ink diffusion in the real world. The method can simulate various tone expressions on different paper types. The effect of mixing strokes from different brush types was also simulated.
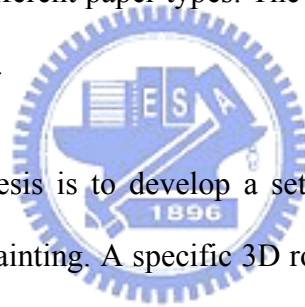
The main goal of this thesis is to develop a set of novel methods for rendering rock texture in Chinese landscape painting. A specific 3D rock model is drawn in outline and with texture strokes using information on the shape, shade and orientation of the model's surface. The main contribution is the modeling and implementation of an integrated framework for rendering rock textures using the traditional brush technique in Chinese landscape painting. The proposed rendering technique involves four main stages. Figure 1 presents the procedure in detail. First, 3D information is extracted for rendering the rock texture. Secondly, the outline of the silhouette is determined. Third, the curvature direction field on the surface is computed and the streamlines for texture strokes are generated. Finally, brush strokes are applied as outlines in the drawing and the rock texture is captured by vertical or slanted strokes along streamlines with a rich ink tone referenced by shading value.

Chapter 3

Chinese Landscape Painting

Chinese ink painting is a traditional art that is over three thousand years old. Chinese ink painting stresses the notion of "implicit meaning" in which painters use a minimum amount of strokes to express their deepest feelings. Chinese landscape painting plays a prominent role in Chinese ink painting. In Chinese landscape painting, rocks are major objects owing to their ability to create the mood of paintings. Artists use the Chinese character *Ts'un*, also meaning wrinkles, to represent texture strokes applied to rock formations. Over the centuries, masters of Chinese landscape painting developed various *Ts'un* techniques, which form the basis of an artist's training. Chinese landscape painting with texture strokes is characterized by the following procedure:

1. An artist begins to visualize a land formation with external contours, which define the overall shape. Internal contour, as added to imply folds on the slopes, reveals the position and direction of the ridge and determines its volume.

2. After the internal contours are defined, texture strokes are applied in the area.

3. Texture stroke is used to symbolize the rock formation.

4. Finally, the brush moves along the path of the stroke and deposits ink on the rice paper.

Of relevant interest is more thoroughly understand Chinese art by analyzing basic rules of Chinese painting. The application of the ink and brush is an essential element of landscape painting techniques. In the remainder of this chapter, the first introduction is the properties of Chinese ink and the four treasures. Besides, six major rock textures are also described in section 3.2.

3.1 Properties of Chinese Ink

Chinese ink painting uses four tools, commonly called the "four treasures"(文房四寶). Figure 3.1 depicts The Four Treasures - brush, ink stick (墨), ink stone (硯台) and paper. They are all used in calligraphy, writing and painting in China. The bristles of the brush touch the surface of the paper, and the ink in the bristles seeps into the highly absorbent paper, creating a stroke whose edge is fluffy and blurred. These characteristics of diffusion represent complex physical phenomena that cannot be accurately simulated by conventional graphical techniques such as texture mapping or degradation functions, since a purely mathematical method generally results in flatly blurred images that are unlike realistic diffusion images.
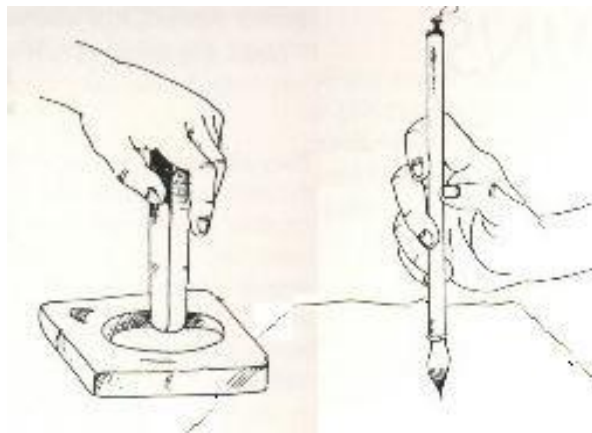
Figure 3.1: the four treasures of Chinese ink painting.

The ink is a kind of colloidal liquid and diffusion phenomena can be considered as typical instances of the diffusion of a colloidal liquid in a highly absorbent paper. The capillary effect importantly causes ink to diffuse into the structure of the paper. Typical paper consists of fibers in random positions and directions; small holes and spaces among the fibers act as thin capillary tubes that carry water away from the area in which it is initially applied, causing diffusion.

Capillary phenomenon, a physical mechanism, is an important factor that causes the ink diffusion in the paper structure. In Figure 3.2, a thin tube is placed in a container filled with water with one end in the water and the other end in the air. The liquid will rise inside the tube and the liquid surface inside the tube is higher than the surface of the outside water. This phenomenon can also be observed in the ink diffusion in paper. The typical paper is composed of fibers which are positioned in random position and random direction in which small holes and spaces between fibers act as thin capillary tubes for carrying water away from the initial area, and create diffusion, as shown in Figure 3.3.
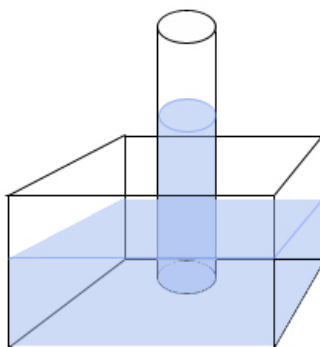
Figure 3.2 : The capillary phenomenon.

Figure 3.3 : The real ink diffusion effect.

Besides the capillarity, the forces that move the ink include interactions among water molecules, water and carbons, and the force due to gravity, among others. The black ink is a dilute mixture of water and colloidal black carbon particles, which diffuse into paper in the absorbed water. Water and carbon are the two main constituents of Chinese ink and the motion of ink in the fibers as simulated as chaotic will be discussed in Chapter 4.

3.2 Rock Texture Strokes (*Ts'un*)

Rocks are primary objects in Chinese landscape painting because of their power to create the mood. Artists use the Chinese character TSUN, also meaning wrinkles, to represent texture strokes when applied to rock formations. Over the centuries, masters of Chinese landscape painting developed various TSUN techniques. In the Tang dynasty, the range of subjects in painting expanded and landscape became established as a distinct category. Chinese landscape painting provided a more spontaneous style that captured images in abbreviated

suggestive forms. Chinese landscape painting has been cultivated by masters through a long evolution, into an exquisite art form.

The Chinese *Ts'un* depicts texture in Chinese painting. *Ts'un* represents a rough, cracked surface. *Ts'un* refers to woven strokes that depict the texture of rocks. According to "The Mustard Seed Garden" (芥子園畫譜), published in 1679, 19 texture strokes were recognized by the time of the Ching Dynasty (清朝). These texture strokes are the most important elements of Chinese landscape painting. Different kinds of texture strokes are used to represent different kinds of mountain. For example, granite mountains which always appear as squares or pyramids, are always painted using *axe-cut* strokes. Meanwhile, sedimentary mountains, which have a striated or layered texture, can be painted using hemp fiber strokes. Topographically, old flat lands are always painted using *hemp-fiber* strokes. When old lands rise up and are cut by rivers, they are treated as new and may be painted using *axe-cut* strokes. Moreover, young land that is eroded by rain and rivers and becomes softer can be painted using *hemp-fiber* strokes and *lotus-leaf* strokes (荷葉皴). All mature texture strokes may be divided into three groups, as follows.

1. Dot texture strokes, including *raindrop* strokes (雨點皴), Mi dots and *half-bean* strokes (豆瓣皴), among others.

2. Line texture strokes, including long hemp fiber strokes, short hemp fiber strokes, lotus leaf strokes and *ox-hair* strokes (牛毛皴), among others.

3. Plane texture strokes, including big *axe-cut* strokes and small *axe-cut* strokes.

Chinese artists use points, lines, planes and brushstrokes to depict nature. A painter of Chinese landscapes must understand both nature and ink brush technique. The proposed

method simulates texture strokes, as will be discussed in greater detail in the chapter 6 and chapter 7.

In the development of texture strokes in Chinese landscape painting prior to the tenth century, the Chinese only used outlines to depict rocks and mountains, but they did not yet use texture strokes. Within the outlines, ink shading was applied. Later artists attempted to substitute ink shading for the texture strokes. Generally, texture strokes are applied using six techniques. Figure 3.4 shows these six kinds of texture strokes painted by Liu [24].

Hemp-Fiber Stroke (批麻皴)

Hemp-fiber stroke, shown in Figure 3.4(a), spreads and weaves like the fibers of the hemp from which it takes its name. The *Hemp-fiber* stroke is one of the most important strokes in Chinese landscape painting. Several texture strokes have been designed from the *hemp-fiber* strokes. The *hemp-fiber* stroke is a long line stroke painted with a dry vertical brush. Numerous long strokes are woven together in a pattern that frequently resembles a fishing net. This stroke imparts a rich, profound and soft feeling and is best used for depicting rough rock surfaces. Developed by the great Southern School master Tung Yuan

(907- 960 AD), the short *hemp-fiber* strokes were varied and generally favored by the literati painters, who dominated mainstream Chinese landscape painting, beginning with the emergence of the Four Masters of the Yuan dynasty (元四大家). The most important of the four Masters, Huang Kung-wang (1269-1354 AD, 黃公望), practiced the strokes in a loose, calligraphic fashion.

Axe-Cut Stroke (斧劈皴)

The *axe-cut* stroke is a slanted stroke used in painting much like an axe is used to cut wood, shown in Figure 3.4(b). The *axe-cut* stroke is excellent for represent smooth cliffs and flat, planar rock surfaces. This stroke dominated Southern Sung (南宋) landscape paintings between the 12th and 13th centuries. Moreover, this stroke is ideal for depicting very hard rock. The *axe-cut* texture strokes developed earlier during the Sung dynasty (宋朝) by Li Tang (1049-1130 AD, 李唐). These simplified yet natural slanted brushstrokes depict earthen forms and hills. The stroke also effectively describes angularly shaped rocks of crystalline quality and sedimentary rocks displaying layered structures. The best-known exponents of the *axe-cut* strokes are Ma Yuan (馬遠) and Hsia Kuei (夏珪), associated with the Northern School of landscape painting, which particularly thrived in the Sung dynasty.

Lotus-Leaf Stroke (荷葉皴)

The *lotus-leaf* stroke was named owing to its similarity to the pattern of veins of lotus leaves, shown in Figure 3.4(c). These veins diverge and divide outwards from a central line many times. The lotus leaf stroke is used to represent mountain ridges or cracks in rocks and is always painted using a vertical brush.

Raindrop Stroke (雨點皴)

This stroke, Figure 3.4(d), is named after the rain because it resembles a *raindrop* that has just reached the ground. This stroke is also known as the sesame stroke, the thorn stroke or the bean stroke. This stroke is applied particularly in the foreground of paintings including

several broken fragments of rock This stroke can be used to depict rocks that have been eroded, and thus have developed pockmarks and holes.

Mi-Dot Stroke (米點皴)

Mi-dot, Figure 3.4(e), is named after the artist who first used this kind of dot, Mi Fu (1051-1107 A.D. 米芾). This dot is particularly good for portraying cloudy mountains and rainy landscapes. This stroke is not only a texture stroke, but can also be used to depict a mountain forest containing several trees. These dots frequently appear horizontally, and therefore are also called horizontal dots.

Boneless Stroke (沒骨皴)

The *boneless* stroke, Figure 3.4(f), is always painted with a wet brush, using slanted strokes. The ink gradation is very soft and differs from other texture strokes which have a strong, hard feeling. This stroke is not good for depicting the texture of rocks, but can successfully provide a three-dimensional feeling and give form and substance to rock. This stroke is good present mountains are in the fog or in the mist.

(a)*Hemp-fiber* Stroke
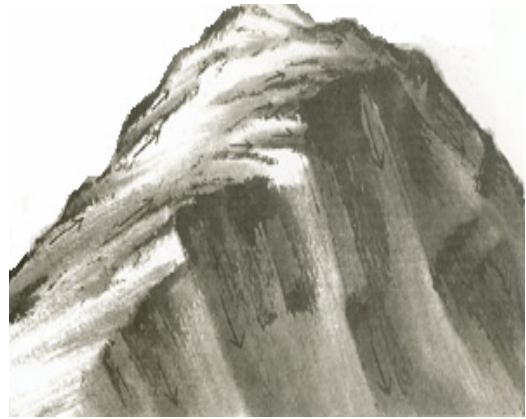
(b)*Axe-cut* Stroke

(c)*Lotus-leaf* Stroke

(d) *Raindrop* Stroke

(e) *Mi-dot* Stroke

(f) *Boneless* Stroke

Figure 3.4: Six Texture Stroke examples in actual Chinese landscape paintings by Liu [24].

Chapter 4
Ink Diffusion Simulation

Simulating the behavior of Chinese ink is challenging work because ink moves in a complex manner. This thesis proposes a new method fo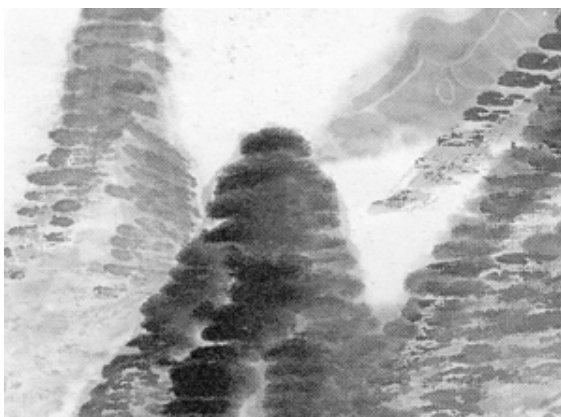r simulating the diffusion of ink in paper. The method is based on a physical mechanism and an observational model of the interaction among real drawing materials used in Chinese ink painting and the variations in the diffusion of ink in the real world. The goal is to capture the core physical properties and behaviors to produce a high-quality ink diffusion model that a painter can use to generate a Chinese ink painting, including brush strokes, in various styles.

The proposed method has the following advantages. First, it simulates the physical behavior of ink diffusion, and can thus generate strokes that exhibit a feathery effect; second, it can blend two strokes with different thickness. Using this method to render a Chinese ink painting can generate highly realistic blending effect

4.1   Discrete Paper Model

Several kinds of paper are used in Chinese ink painting. Basically, papers have one of two types of fiber mesh. The first kind is a regular fiber mesh, such as in silk paper, whose fibers are uniformly aligned as woven. The second kind is an irregularly distributed fiber mesh, such as in Hsuan paper that consists of a mesh of randomly positioned fibers.

Constructing a mesh like Hsuan paper requires an appropriate data format in which to represent a mesh structure. Traditionally, a network format is used to represent paper with a random fiber network [10]. The continuous interaction between water and fiber is discretely simulated by computers; a two-dimensional array, whose entries specify the attributes of the structure of the mesh, is used. The entire mesh in the paper is separated out into many layers, each of which are divided into [X×Y] cells called papels (paper element) [20]. A papel is a basic unit of paper structure and corresponds to a pixel.

Capillarity is evident in paper modeled as interlaced fibers. The ink seeps into the paper and is then pulled away from the area of application by capillary attraction; it then travels through the fibers. Some of the diffused ink is deposited in the holes or spaces between the fiber through which it passes; the remaining ink continuously flows along the fibers until it is completely absorbed.

Let Absorbency(p) of papel p be defined as follows. When the moving ink passes through p with N fibers, the amount of water deposited in p is Q. The relationship between Q and N can be expressed as $Absorbency(p) \propto N \propto Q$. Based on this relationship, several models of paper can be defined with various absorbency, by fibers with various densities. An equation for the absorbency of each papel is,

$$Absorbency(p) = Base + Var \times rand() \qquad \ldots (4.1)$$

Figure 4.1 depicts the resulting ink diffusion in three types of paper with different absorbencies. The coefficient of absorbency is a real number between zero and one.

| (a) 0.1 | (b) 0.4 | (c) 0.7 |
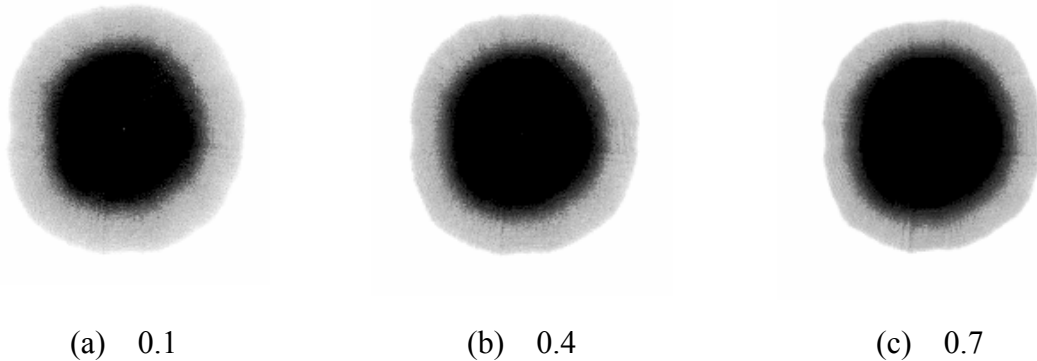
Figure 4.1: Three simulated ink diffusion image represent different kinds paper with different degree of absorbency value.
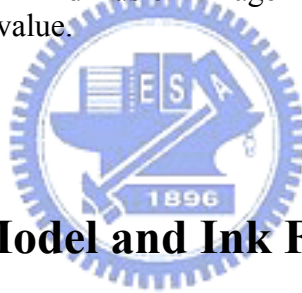
4.2   Discrete Ink Model and Ink Flow

4.2.1 Water Particles

Water is a liquid which can move to anywhere in the paper under the forces associated with capillary action. All water particles are defined as objects with the same volume, mass, color and respond to forces. They only differ in position, recorded as coordinates in the papel. The quantity of water accordingly governs the span of the diffusion image or the number of diffusion steps. When the water in a certain papel flows out, its quantity and direction must be determined.

Based on above description, the approximate equation for K(p), the ratio of the quantity

of out-flowing water to the quantity of water in the papel p is represented as,

$$K(p) = F_{base} + F_{diff} \times \left(1 - \left(1 - Absorbency(p)^2\right)\right), \quad \dots (4.2)$$

Where F_{base} is a real number between zero and one that represents the basic flow rate p, and F_{diff} is a real number between zero and one that represents the difference between the highest flow rate and the lowest.

The quantity of water that flows in all the directions to neighboring papels is determined by associated probabilities. Section 4.3 discusses the estimation of the probability associated with each direction of water flow.

4.2.2 Carbon Particles
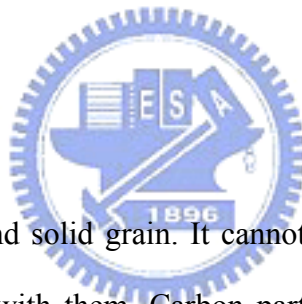
A carbon particle is a black and solid grain. It cannot move by itself. When water particles move, carbon particles move with them. Carbon particles are suspended and move in this liquid since they collide with water particles. Suspended carbon particles undergo Brownian motion, buffeted water particles.

The carbon particles can be most simply simulated like water particles. They have mass, position, diameter and color. These attributes all vary among particles. The diameter and mass of a carbon particle are determined by the fineness to which the ink is initially ground. If the ink is initially ground coarsely, it contains small and large particles that produce observably different color intensities at the border of the initially brushed area. However, most homogeneous, small and uniform carbon particles move in water unhindered by the fibers, such the intensity changes smoothly over across the diffusion area.

Only carbon particles that are smaller than the space between the fibers can seep into the mesh in the water. Particles larger than the space remain in their initial positions, as shown in Figure 4.2. This phenomenon is referred to as the "filtering effect" of the fiber mesh, and can be represented as follows, where p is the papel in which the carbon particle is located.

if (Carbon_Diameter > Hole_Diameter(p)) then
  Carbon_Position ← p
else
Carbon_Position ← Water_OutFlow_Direction(p)

In Figure 4.2, two adjacent cubes represent two neighboring papels. Black grains in papels are carbon particles with different sizes. It is chaotic between two papels represent fibers. The arrow represents the direction in which the water flows; the carbon particles move in this direction. Larger carbon particles cannot pass through holes in the paper.
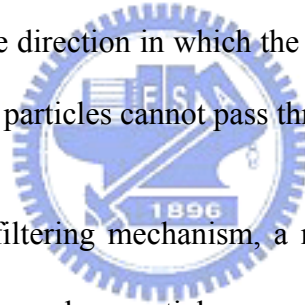
As well as the diameter-filtering mechanism, a mass-filtering mechanism is proposed. Suppose V_c is the velocity of a carbon particle c, suspended in water in papel p, and W_p is the quantity of out-flowing water from p. The relationship between V_c, W_p and the diameter of holes in p, Hole_Diameter(p), is given by $V_c \propto W_p$, $V_c \propto \frac{1}{(Hole\_Diameter(p))^2}$. If carbon particle c is too heavy to exit papel p and is deposited in p, then $V_c \leftarrow 0$. Accordingly, an upper-bounded threshold T_p for papel p determines whether the carbon particle can. If the mass of carbon particle c exceeds T_p then $V_c \leftarrow 0$. The value of T_p is determined by depending V_c. The relationship between T_p and V_c is represented as,

$$T_p = T(V_c) = T(W_p \times \frac{1}{(Hole\_Diameter(p))^2}), \quad \ldots\ldots (4.3)$$

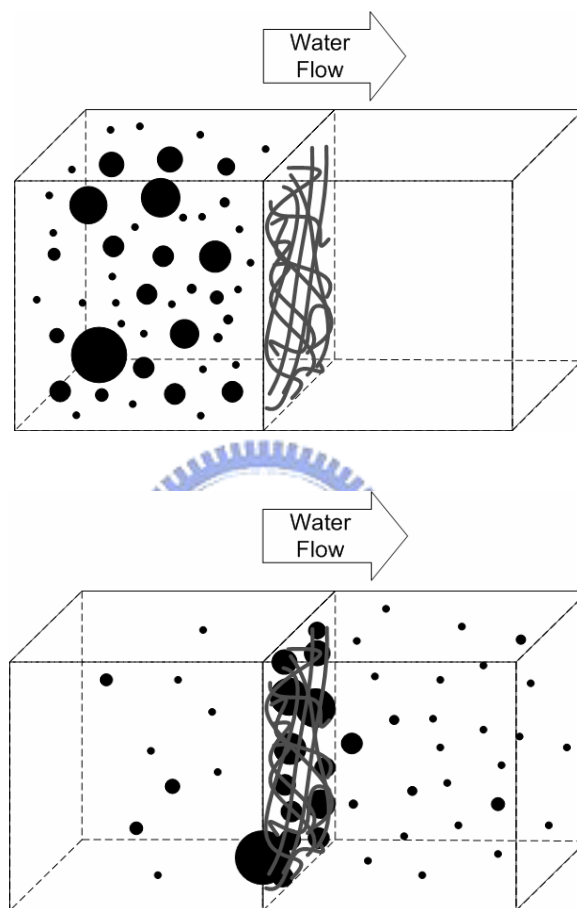where T a transformation from V_c to T_p.

Figure 4.2: An illustration to explain the phenomenon called "*filter effect*".

4.3   The Moving Direction of Water Flow

Water may flow from one papel to some of its neighboring eight papels. The directions of this motion are determined by considering the following factors that dominate the flow of water.

1.   Gradient of water between neighboring papels, based on *Brownian* motion.

2.   Absorbency of neighboring papels for water.

3.   Paper texture of neighboring papels.

4.   Inertia of water.

Figure 5 shows that a papel C_0 has eight neighboring cells p_k defining eight directions, d_k (k = 1, 2,, 8). The probabilities of motion in each direction are calculated according to the above four factors. The amount of water particles that flow into a neighboring papel is proportional to the calculated probability.
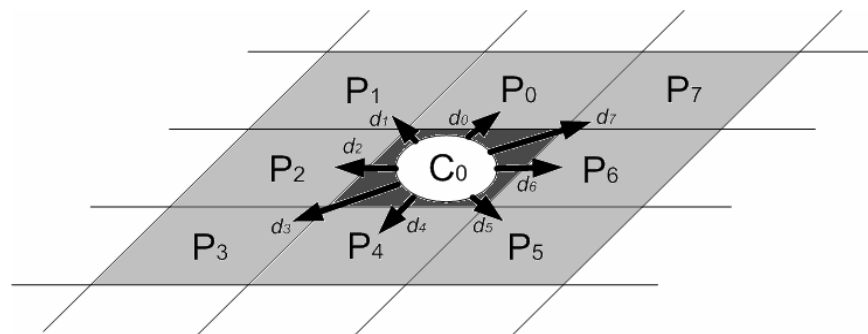

Figure 4.3: Determine directions of water flowing into neighboring papels, p_k (k = 1, 2, , 8), according to the probabilities in eight directions calculated based on four factors.

4.3.1 Gradient

The motion of water particles in paper is assumed to obey Brownian motion. A mixture of two sets of different numbers of water particles will produce irreversible diffusion in which water particles are transferred from the set with more to that with fewer particles. This movement continues until the difference between the numbers of particles in the two sets reaches a value that expresses the balance of forces on these two sets. Gradient represents the difference between the numbers of water particles in the two sets.

The number of water particles in c_0 and p_k are assumed to be W_c and W_k, respectively. The probability, based on Brownian motion, is determined by the equation,

$$G_k = \frac{u(W_c - W_k)}{G_{sum}}, \quad G_{sum} = \sum_{i=1}^{8} u(W_c - W_i) \quad \text{........} \quad (4.4)$$

where G_k is a probability determined by gradient. $u(x)$ is the unit function; that is, if $x \geq 0$, then $u(x) = x$, otherwise $u(x) = 0$.

4.3.2 Absorbency

Attraction to each neighboring papel causes different amounts of water to flow into each. Newton's Second Law of Motions is: $f_d = M \times a$ (4.5)

The dynamic friction f_d is ideally a constant force between the flowing water and the fibers. The term a is the acceleration of the flowing water particles. Based on the theorem of Theo, a is usually much smaller than g, the acceleration due to gravity. Therefore, it can

be regarded as constant. M is the mass of the flowing water particles. The pre-defined uniformity of the mass of water particles is such that the amount of flowing water is proportional to M. Assume N_w is the number of water particles in the flowing water.

From Eqs. (4) and (5), $f_d \propto N_w \times a$. This important deduction indicates that N_w increases with f_d. Based on the relationship in Eq. (3), $f_d \propto a_p$ ➔ $N_w \propto a_p$, where a_p is the absorbency of papel p. Assume that the eight neighbors of the central papel c_0 are p_k, and the absorbency of c_0 and p_k are $Absorbency(c_0)$ and $Absorbency(p_k)$, respectively. Probabilities, based on absorbency, are attributed to the eight directions according to,

$$A_k = \frac{Absorbency(p_k)}{A_{sum}}, \quad A_{sum} = \sum_{i=1}^{8} Absorbency(p_i) \quad \ldots\ldots(4.6)$$

where A_k (k = 1, 2,, 8) is a probability based on absorbency.

4.3.3 Paper Texture

The texture of the paper also determines the directions in which the water flows. When water undergoes capillary action and flows in the holes among the fibers, fibers in the trajectory of the flowing water become saturated. Variously aligned of fibers promote different trajectories of the flowing water. Two kinds of paper exist – one with regular and the other with an irregular fiber mesh, such as silk paper and Hsuan paper, respectively.

Papers with differently distributed fibers have different textures. When the water

particles in a papel c_0 flow out, c_0 is the center of a 3×3 texture mask, M_{direct}, with a central element m_0 at c_0. The eight elements at the periphery of M_{direct}, m_k (k = 1, 2, …, 8), are assigned weights to represent the alignment of the fibers.

4.3.4 Inertia

Besides the three aforementioned factors, inertia is involved in another important physical mechanism. According Newton's First Law of Motion, inertia increases with the mass of an object. During painting, water is treated as a moving object. Assume that water in papel p_0^t in the (t)-th time interval originates from papels p_k^{t-1} in the (t-1)-th time interval, and the quantity of water particles flowing in the direction d_i^{t-1}, from p_k^{t-1} to p_0 is w_k^{t-1}. Based on the relationship between inertia and the mass of an object, water in p_0^t will flow out in the same direction as w_k^{t-1}. The probabilities associated with the eight directions of flow from p_0^t, I_k^t, are proportional to the w_k^{t-1} in direction d_i^{t-1}.

The probabilities are used to determine the directions of water flow. A higher probability of a neighboring cell corresponds to more water's flowing into it. The probabilities are,

$$R_k = \frac{\alpha_1 G_k + \alpha_2 A_k + \alpha_3 m_k + \alpha_4 I_k^t}{R_{sum}}, \quad R_{sum} = \sum_{i=1}^{8} (\alpha_1 G_i + \alpha_2 A_i + \alpha_3 m_i + \alpha_4 I_i^t)$$

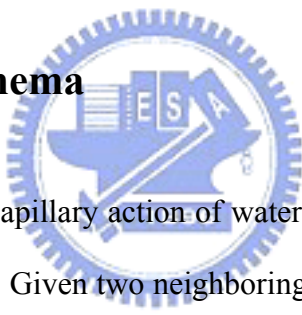(7) where R_k (k = 1, 2, …, 8) is the probability governed by four main factors for each neighboring papel and α_1, α_2, α_3, and α_4 are weights that control the behavior and movement of water, resulting in different kinds of effects.

The directions of the water particles, the points in the mesh to which water will flow are determined using these probabilities. The quantity of water that flows to neighboring papel p_k (k = 1, 2, …, 8) is proportional to the probability R_k.
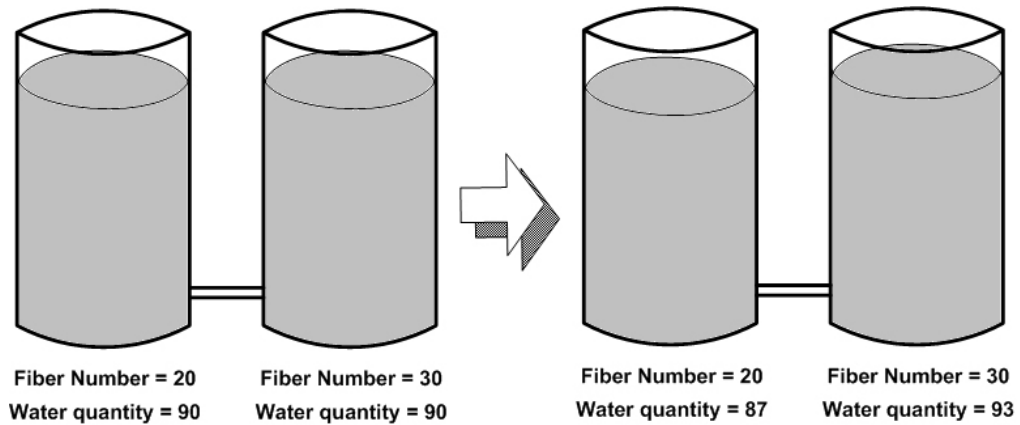
4.4 Ink Diffusion Process

The diffusion of ink in paper is complex. It can be regarded as a continuous and time-dependent.   The evaporation of water and the absorption of any ink left on the surface of the paper are also considered.

4.4.1 Ink Diffusion Schema

Ink diffusion is caused by the capillary action of water between fibers and the gradient of the quantity of water in paper cells. Given two neighboring papels saturated with water, as shown in Figure 4.4(a), as a rough estimate, only the strength of the capillary forces in these two papels influences the direction of flow of the water. In contrast, in Figure 4.4(b), only one papel is saturated with water and the other is absolutely dry. The water gradient between these two papels is maximal, resulting in an obvious propagation of water from the papel with much to the other with little.

Fiber Number = 20   Fiber Number = 30   Fiber Number = 20   Fiber Number = 30
Water quantity = 90   Water quantity = 90   Water quantity = 87   Water quantity = 93

(a)

Fiber Number = 20   Fiber Number = 30   Fiber Number = 20   Fiber Number = 30
Water quantity = 90   Water quantity = 30   Water quantity = 58   Water quantity = 62
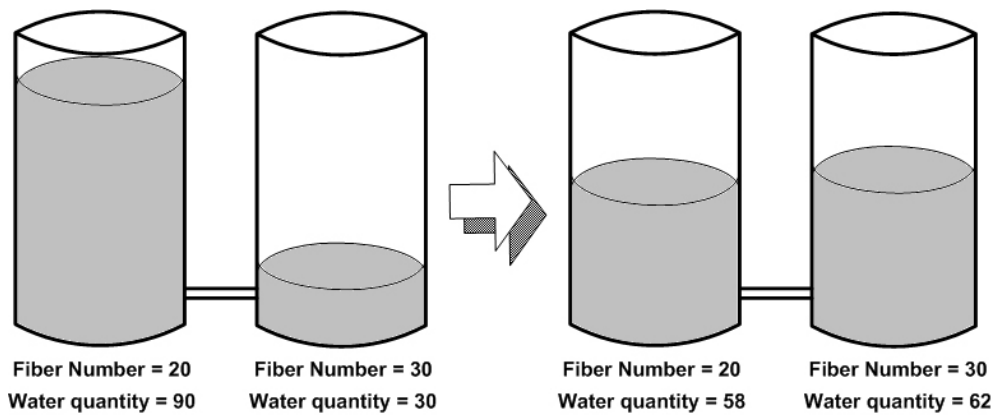
(b)

Figure 4.4: Two illustrations are given to describe the water propagation influenced by capillary force and gradient of quantity of water, relatively. Two containers with a pipe connecting to each other in this picture represent two adjacent papels.

Besides, three issues were addressed in simulating ink diffusion - brush strokes, initial area and propagation. The area on the surface of the paper touched by the brush is approximately circular, because the profile in the horizontal direction of the brush used in Chinese Ink Painting is round. The stroke is a sequence of circular segments shown in Figure 4.5. Ink in old segments starts to diffuse earlier than in new segments, and ink within old segments may even dry up. Stroke segmentation makes the simulation of the painting

processes more realistic. The skeleton of a brush stroke area of the application of ink is just one line, and can be simply used to describe a brush stroke as a trajectory of the center of a circle.
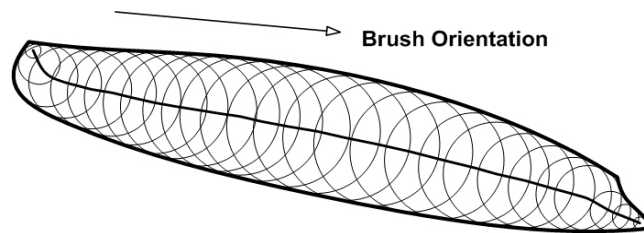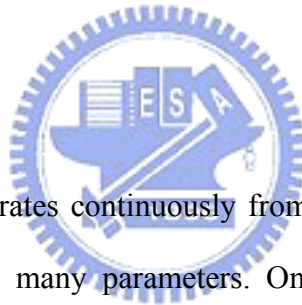

Figure 4.5: An example of Stroke segmentation. The stroke is divided into circular segments with their center positions on a given curve.

4.4.2 Evaporation

In the real world, water evaporates continuously from paper. The evaporation of water is a complex process governed by many parameters. One important parameter is the area of contact with the atmosphere. When other parameters are fixed, a larger contact area increases the rate of water evaporation. Assume that the contact area of each papel with atmosphere is the same. The rate of evaporation from each papel is then approximately equal.

Important parameter humidity resists the evaporation of water. For simplicity, assume that the number of water particles evaporated from papel P ion the t-th step, E_p^t, depends on the humidity H ($0 \leqq H \leqq 1$) according to the equation $E_p^t = h(1-H) \times Water_p$, where $Water_p$ is the number of water particles in papel P, and function $h(x)$ yields a coefficient for the evaporation of water, where $0 \leq x \leq 1$.

4.4.3 Refilling Ink

When the brush's bristles first touch the initial area, the paper does not completely absorb the ink pulled out by capillary action from the bristles in a single time step. The rates of absorbency and capillary action are not sufficiently high to prevent ink from remaining on the surface of paper. Some of this remaining ink saturates a papel in the next time step. This phenomenon of saturation by remaining ink, called ink refilling, occurs continuously in the subsequent time steps. Ink refilling is promoted by adding ink to the papels in the initial area stepwise at a certain rate until the remaining ink on the surface of paper has been exhausted.

4.4.4 Intensity of Paper Cells

A papel contains water particles and carbon particles. Water particles are achromatic. Carbon particles are defined as absolutely black. On the gray scale, each carbon particle is zero. Accordingly, the color intensity of the paper is determined by the color of the fibers of the paper and the density of carbon particles. Assume C is the number of carbon particles in papel P, and the maximum capacity of the carbon particles of P is C_{max}. The color intensity CI_p in P can be calculated from $CI_p = 255 \times \left(1 - \dfrac{c}{c_{max}}\right) - P$, $P = 255 - PI_p$ where PI_p is the original color intensity of paper.

4.5 Experimental Results

The proposed method yields several results. Figure 4.6 shows the simulated dropping of ink onto Hsuan paper. The time required for the simulation is also given. Figure 4.7 depicts an example of the basic blending of two brush strokes. The process of "dense brush following dilute brush" is described as follows. After a dilute brush stroke is applied to the paper, a dense brush stroke is immediately applied to the same area, before the first stroke has dried.

(a) 10 steps, 8 sec   (b) 20 steps, 22sec   (c) 30 steps, 39 sec   (d) 40 steps, 63 sec
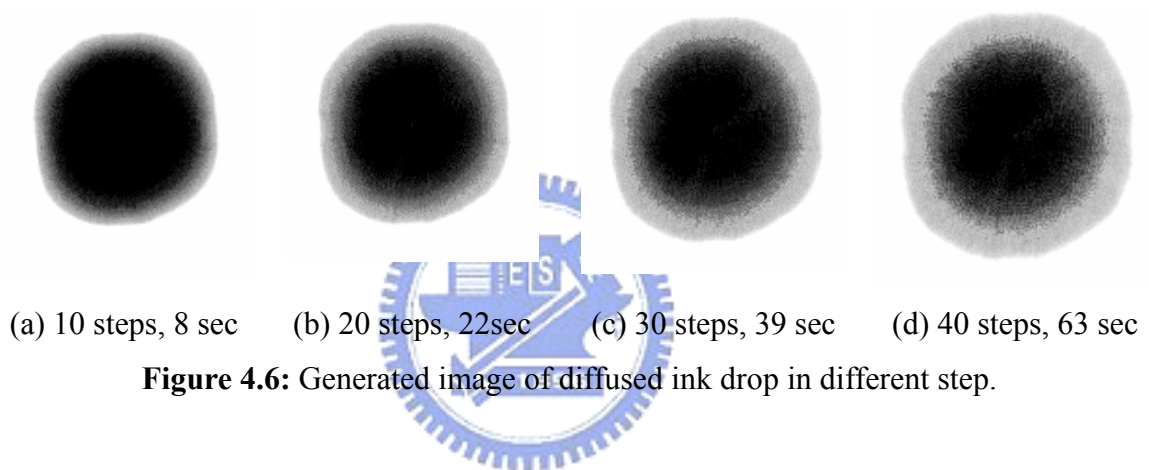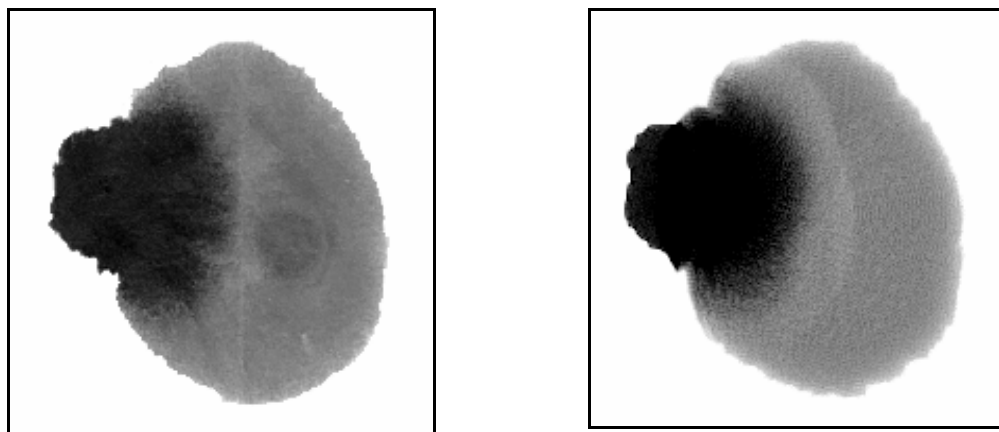
Figure 4.6: Generated image of diffused ink drop in different step.

(a) Actual ink diffusion   (b) Simulated ink diffusion

Figure 4.7: (a) Actual ink diffusion image on Hsuan paper, (b) Simulated ink diffusion image.

Chapter 5
Brush Strokes Generation

A beginner in Chinese painting must learn some technical terms and make a preliminary study of brush techniques. A stroke may be light or heavy. When drawing a line, a painter may half-lift the brush such that only the tip touches the paper, to make a swift and thin line. He may, as the subject requires, press the tip of the brush onto the paper to make a thick, heavy line. Sometimes, he stops and changes the direction of the line, inserting a break into the brush-stroke. A line may therefore look smooth or rugged or may even include some blank spaces, deliberately made by not putting enough ink onto the brush-tip. Various brush-strokes suggest different textures. Two fundamental brush strokes, the vertical stroke and the slanted stroke, are simulated.

5.1   Virtual Brush Model

The application of the brush is an essential element of landscape painting techniques. Brushwork is very important in Chinese ink painting. A brush consists of a bundle of bristles. Where the brush contacts the rice paper, the footprints of the bristles form a contact region.

While painting, these bristles deposit ink on the circular region in contact with the rice paper, as shown in Figure 5.1.
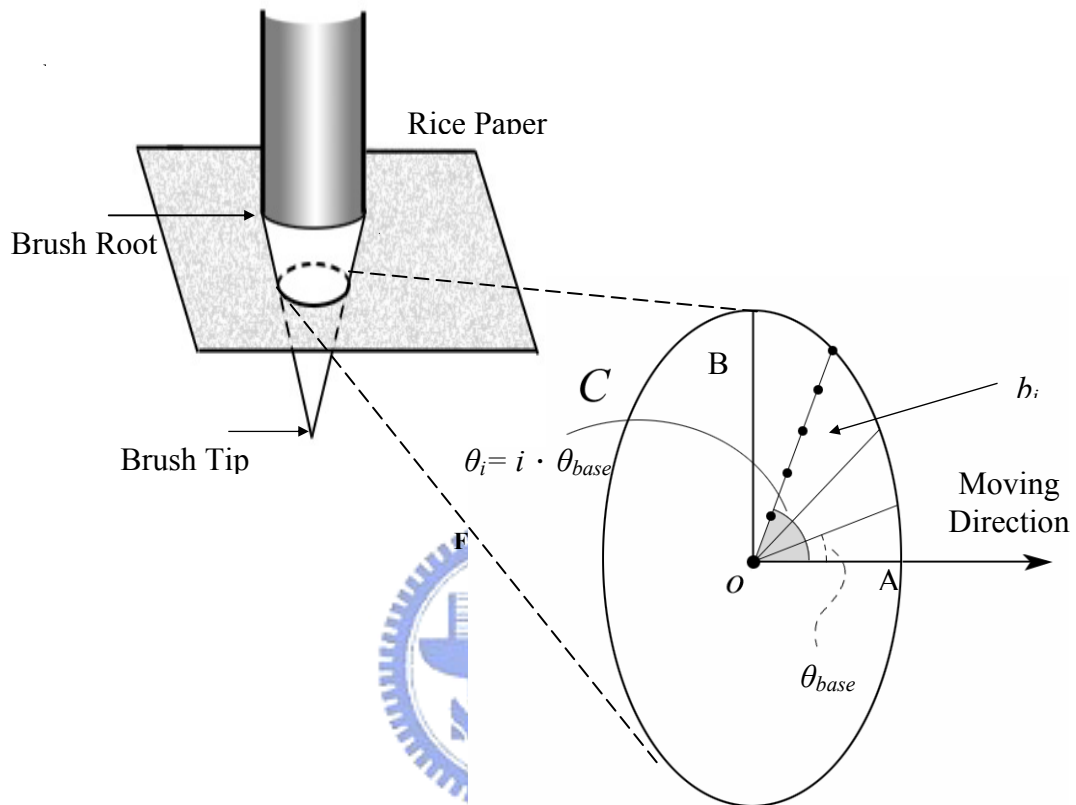

Figure 5.1: Virtual Brush Model

The contact region is a 2D ellipse. Consider in Figure 5.1, an ellipse C, with center o, as the contact region between the brush and rice paper. A and B are the short axis and long axis of C, respectively. A set of bristles is distributed inside the circle. We denote each bristle as bi, and represent it in polar coordinates with respect to the center of the ellipse C.

$$b_i = (d_i, \theta_i) \quad \dots\dots\dots\dots\dots\dots\dots\dots\dots\dots\dots\dots\dots(5.1)$$

where i is the bristle index. d_i is the distance from o to b_i. θ_i is the angle between x-axis and $\overline{ob_i}$. Herein, the central angle of C is split equally to obtain the base angle, θ_{base}, such that θ_i

is $i \cdot \theta_{base}$. For each θ_i, we locate the number of bristles on the radius. Two parameters allow the number of bristles to be controlled: one is the base angel θ_{base}, and the other is the number of points located on the radius. A smaller base angle and more located points both result in more bristles. Parameters may be adjusted to obtain different brush sizes and resolutions.

5.1.1 Motion Mechanism

During painting, the contact region moves along the stroke trajectory and deposits ink to generate strokes. The stroke trajectory is constructed by Cardinal spline. The curve may be interpolated between two neighboring control points. The center of the contact region travels along these interpolated points, leading circumferential bristles and leaving footprints on the rice paper. Assume the center of the contact region on the rice paper is (O_x, O_y). The position of bristle b_i is given by Equation (5.1):

$$b_{i,x} = o_x + b'_{i,x} = o_x + [d_i \cdot \cos\theta_i - d_i \cdot \sin\theta_i]$$
$$b_{i,y} = o_y + b'_{i,y} = o_y + [d_i \cdot \sin\theta_i + d_i \cdot \cos\theta_i] \quad \ldots\ldots(5.2)$$
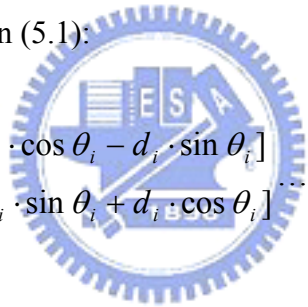
where $b_i = (b_{i,x}, b_{i,y})$. The width of the strokes is controlled by the axial lengths of the contact region, specified at each control point. The axial lengths of interpolated points are linearly interpolated between two neighboring control points.

During painting, brush orientation continuously changes, and brush orientation is an important parameter. Consider Figure 5.2. When the brush moves from point (x_i, y_i) to point (x_{i+1}, y_{i+1}), the moving orientation is determined by the tangent of (x_i, y_i) on the track. In a discrete environment, orientation can be approximated by:

$$T(x_i, y_i) = \frac{y_{i+1} - y_i}{x_{i+1} - x_i} \quad \ldots\ldots\ldots\ldots\ldots\ldots\ldots\ldots\ldots(5.3)$$
$$\theta = \tan(T(x_i, y_i))^{-1}$$

where $T(x_i, y_i)$ is the tangent of (x_i, y_i). Bristles in a contact region are rotated by θ with respect to the center of the contact region. The equation giving the new coordinates of the

bristles is derived from Equation (5.2):

$$b_{i,x} = o_x + [b'_{i,x} \cdot \cos\theta - b'_{i,y} \cdot \sin\theta]$$
$$b_{i,y} = o_y + [b'_{i,y} \cdot \sin\theta + b'_{i,y} \cdot \cos\theta] \quad \ldots\ldots\ldots\ldots(5.4)$$
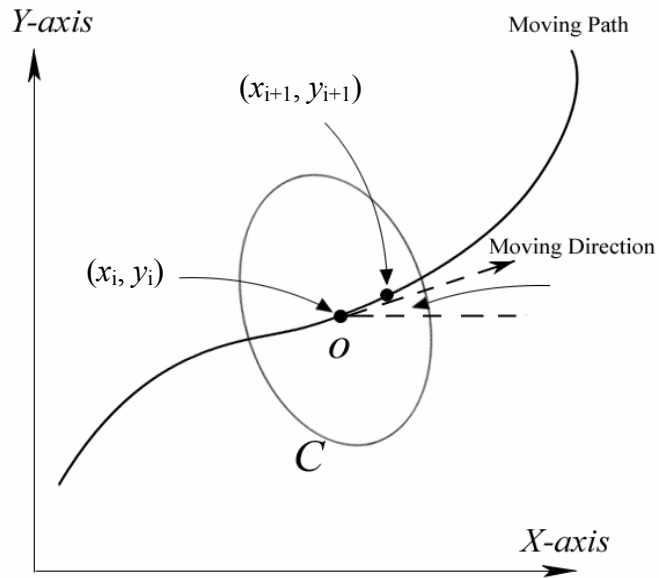

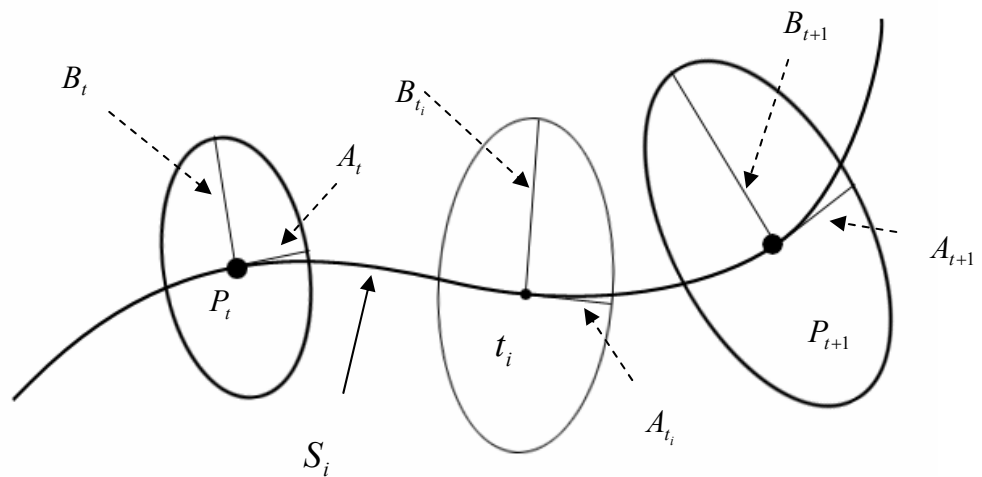**Figure 5.2:** Brush rotates to follow the moving direction.

Figure 5.3: To generate contact region axes with linearly interpolation.

5.1.2 Ink Effects

To present rock textures in Chinese landscape painting, more parameters are required to describe ink effects.

Ink Decreasing (λ_1) : Ink quantity decreases as the brush moves along the rice paper. Thus, less ink is deposited on the rice paper.

Ink Soaking Variation (λ_2) : The concentration of ink in the brush varies, due to the ink itself or the action of the painter. Ink concentration is linearly interpolated in the contact region.

Bristle Material (ρ) : Generally, bristles are made of animal's fur (e.g. Sheep or wolf). A random number added to each bristles. The variance of distribution of the random number is lower to express softer bristles, whereas the variance is larger to express harder bristles.

Bristle Dry-Out (Δd) : Painting with a dry brush may cause bristles to run out of ink and leave gaps along the trajectory of the brush, due to fast evaporation.

Wet Effect (μ) : Water quantity determines the gradient of the ink. The dry brush makes strokes rougher, whereas the wet brush creates more smooth strokes.

Ink Blending: Since absorption has an important effect on painting. Ink blending is conveniently expressed in gray scale, from 0 to 255 black to white. The blending equation is

$$inkNew = inkP \cdot \frac{inkB}{255} \quad \text{...........................(5.5)}$$

where *inkNew* is the ink value after blending, *inkP* is the ink value before blending, and *inkB* is the ink value of the brush.

5.2 Vertical Stroke Technique

When applying a vertical stroke, a painter must hold the brush steady and erect, with the core of brush always in the middle of the brushstroke. This stroke is generally used to define an outline or to make dots and flips. Figure 5.4 displays an example of vertical brush.
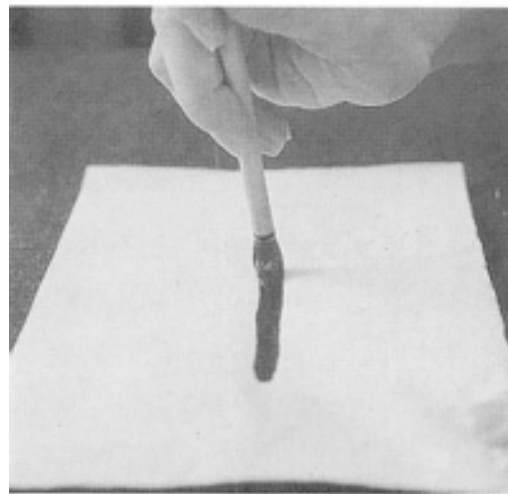

Figure 5.4: Vertical Stroke

A method for painting long, continuous curves using a vertical stroke is presented here. The stroke is applied using a precise and flexible Cardinal spline. The Cardinal spline is an interpolated but not approximated curve, which passes through all specified control points. Feature points of strokes can be selected as control points. The other benefit of the Cardinal spline is its flexibility. Strokes can be painted soft or hard. The cardinal spline enables slackness to be controlled by adjusting parameter t. A smaller t implies a slacker curve. Figure 5.5 plots the precision and flexibility of the Cardinal spline.

When painting strokes, painters normally slow the motion of the brush and change the pressure applied to the brush to capture the verve of a rock. Pressure P varies from zero to one. This pressure determines whether bristles touch the rice paper. It also determines the amount

of ink deposited. For each bristle, b_i, the pressure weight W_p, is defined by,

$$W_p = \begin{cases} 0 & , \quad if \quad \dfrac{\left|b_i' - B\right|}{2 \cdot B} \geq P \\ \left(\dfrac{\left|b_i' - B\right|}{2 \cdot B \cdot P}\right) \cdot (P-1)+1, & if \quad \dfrac{\left|b_i' - B\right|}{2 \cdot B} < P \end{cases} \quad \ldots\ldots\ldots\ldots(5.6)$$

where b_i' is the coordinate of b_i in the contact region, and B is the long axis of the ellipse contact region. According to Eq. (5.6), a specific bristle deposits different amounts of ink as P changes. Figure 5.6 shows different values of pressure and the corresponding stroke styles obtained using the Cardinal spline.
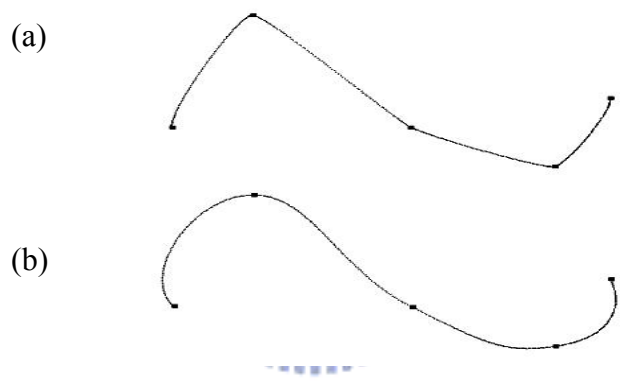

Figure 5.5: Cardinal Curves with different t.
(a) Hard rock's contour ($t = 0.2$).
(b) Soft rock's contour ($t = -0.5$).

Figure 5.6:   (a) Pressure on turning points $= 0.6$.
(b) Pressure on turning points $= 0.8$.

5.3   Slanted Stroke Technique

The slanted-stroke is used when the handle of the brush is tipped to one side and the brush-point lies on the brim of the brush-stroke. It is generally used for wrinkling, daubing and washing. The core and the side of the brush, however, are usually jointly used to convey the nature and form of various subjects. The brush is held and the handle of the brush allowed slanting to one side; the brush-point is on the brim of the brush-stroke. Large slanted strokes can be applied by holding the handle farther from the brush, as depicted in Figure 5.7.

Figure 5.7 : Slanted Strokes.

5.3.1 Pressure Function

The pressure function is the most important factor of the slanted stroke and determines the number of bristles that touch the rice paper and the quantity of ink deposited. We construct the basic pressure function as shown in Figure 5.8.
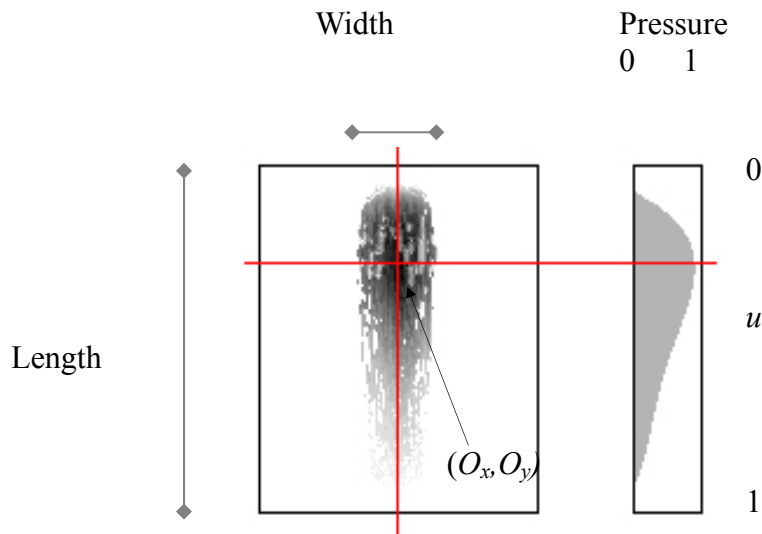
$P(u) = u(1-u)(a_1(1-u)^2+b_1(1-u)+c_1)\ldots\ldots(5.7)$

Figure 5.8: Single Slanted Stroke.

Where u is transferred from the length of the slanted stroke to (0,1), a_1, b_1 and c_1 are constant. The value of P(u) lies between 0 and 1. The pressure is 0 at both the start point and the end point. The center of the slanted stroke is at (O_x, O_y).
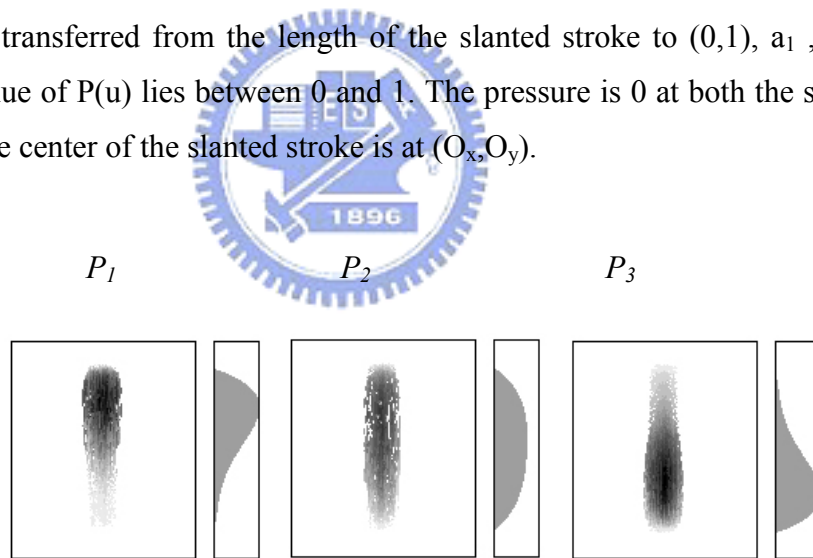

Figure 5.9: Pressure functions of *axe-cut* stroke.

$P_1 = u(1-u)(a_1(1-u)^2 + b_1(1-u) + c_1)$

$P_2 = u(1-u)$

$P_3 = u(1-u)(a_3 u^2 + b_3 u + c_3)$

$Pressure = K_1 P_1 + K_2 P_2 + K_3 P_3$ ……. (5.8)

Generally, changes of pressure are very complex in painting. The other two pressure

functions P_2 and P_3 can also be constructed. Finally, the pressure function is combined with P_1, P_2 and P_3. (Figure 5.9)

5.3.2 Discontinuity

A brush dries out when the amount of deposited ink is under a threshold. Two directional discontinuity factors, one is horizontal and the other is vertical to simulate this effect. The maximum gap size is predefined for vertical directional discontinuity. Once a bristle deposits ink discontinuously, the corresponding gap size can not exceed the maximum gap size. The gap size decreases until it equals zero during the brush moving. A random number is defined for each bristle in the horizontal directional discontinuity, and is added to the ink concentration in the bristle, making the ink color darker or lighter. The discontinuity is also dependent on bristles' material and wet effect.

5.3.3 Experiment Examples

Many styles of slanted strokes can be generated according to the above parameterization. Figure 5.10 displays about ten slanted strokes and blending effect. Strokes with the same pressure indicated on the left are shown in the same row. Table 5.1 lists the corresponding parameter's value.
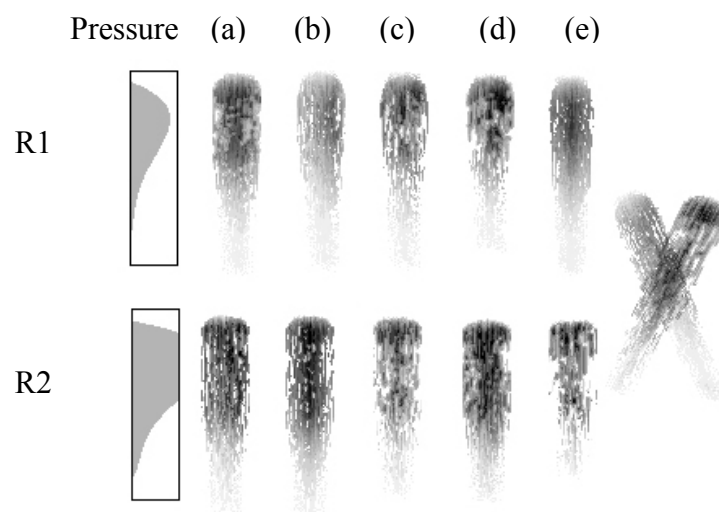

Figure 5.10: Ten slanted strokes and blending sample.

Table 5.1: The corresponding parameters of Figure 5.10.

		(a)	(b)	(c)	(d)	(e)
R1	λ_1	0.6	0.23	0.6	0.8	0.6
	λ_2	0.3	0.4	0.6	0.8	0.4
	ρ	7	6	12	10	6
	Δd	46	36	61	65	25
	μ	80	130	130	100	150
R2	λ_1	0.6	0.5	0.5	0.5	0.36
	λ_2	0.3	0.5	0.3	0.5	0.34
	ρ	12	6	14	18	30
	Δd	47	47	76	36	100
	μ	170	170	100	100	124

Chapter 6

Texture Strokes Synthesis from 2-Dimension Picture

In Chinese landscape painting, painters cluster various strokes to depict stuff of rock surfaces. The different rock textures are generated by changing stroke distribution, ink density, stroke length, and something else. In our approach, the knot and exclusive region are used to control the distribution and density of strokes. In this chapter, we introduce several parameters: length, crossing angles, and perturbation. Stroke styles are presented with the three parameters. With different combinations of spatial and style parameters, users can generate various *hemp-fiber* strokes and *axe-cut* strokes.

Hemp-fiber and *axe-cut* are two major types of texture strokes, shown as Fig 6.1 and Fig 6.2. A slightly sinuous and seemingly broken line, the *hemp-fiber* stroke is used for describing the gentle slopes of rock formations whereas the *axe-cut* stroke best depicts hard, rocky surfaces. This chapter presents a novel method of synthesizing rock textures in Chinese landscape painting, useful not only to artists who want to paint interactively, but also in automated rendering of natural scenes. The method proposed underwrites the complete painting process after users have specified only the contour and parameters.

Figure 6.1: *Hemp-fiber* texture strokes by Huang Kung-wang.

Figure 6.2: *Axe-cut* texture strokes by Hsia Kuei.

6.1 Texture Strokes Area

The area surrounding the texture strokes is a region where only one style of rock textures is applied. In addition, an area surrounding the texture strokes is equipped with a painting mesh, which consists of 10×10 grids, to control the orientation and distribution of texture strokes. There are three steps for making a painting mesh as follows: (1) corner vertices adapt ion, (2)

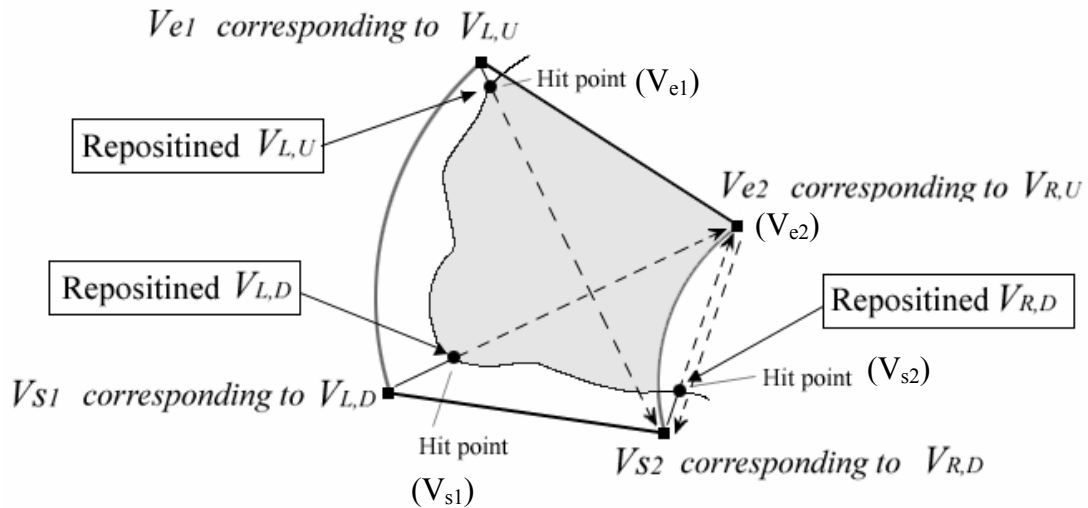boundary vertices interpolation, and (3) interior vertices generation.

Figure 6.3: The process of corner vertices adaption.

According to four user-specified points, the corner vertices of painting mesh can be obtained in the region of the rock. Figure 6.3 shows the four point V_{LU}, V_{LD}, V_{RU}, and V_{RD}, which are specified by user. Where V_{e1} is the repositioned point of V_{LU} with the intersection of line $\overline{V_{LU}V_{RD}}$ and Cardinal path of rock contour. By the same way, the other three corner vertices can be found. In step 2, there are nine boundary vertices obtained by interpolating the positions of each pair of neighboring corner vertices. Finally, using vector operation to obtain the interior vertices. Since the painting mesh is subdivided into 10×10 grid uniformly, the blending function is linear. Figure 8 shows the process. After step 3, a painting mesh wraps up the actual-painting region tightly.

According to Figure 6.4(d), although an area surrounding the texture strokes encloses a region, the texture is applied inside the rock contour that is grayish color. Coordinates of each grid point of a painting mesh are mapped to the region where textures are applied.
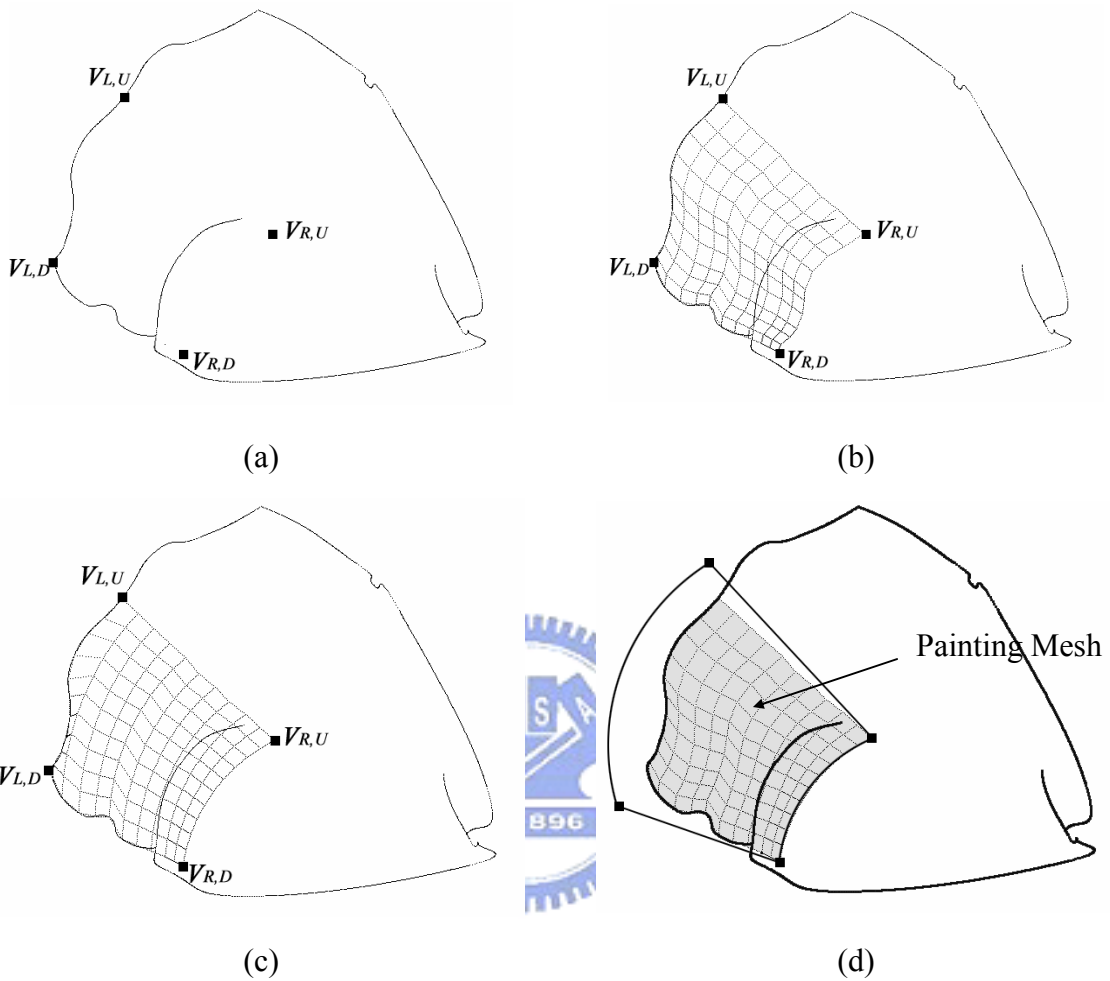
Figure 6.4: The texture strokes area and painting mesh.

(a) The positions of corner points after step 1.

(b) Interior vertices generation according to left side.

(c) Interior vertices generation according to right side.

(d) The painting mesh after blending (b) and (c).

6.2   Distribution and Density

In our approach, the distribution and density of strokes are taken as spatial parameters. They present illumination effects, which make the painted rock stereo. Dense strokes are applied to dark rock surfaces and sparse strokes are applied to bright rock surfaces. Moreover, knot and exclusive region are used to control both of them. Consider Figure 6.5. A knot can generate one or two strokes. If a knot generates two strokes, they cross each other at the knot. Control points are specified at each square overstretched by the strokes in the painting mesh. A set of knots is then placed in the painting mesh, subsequently generating strokes to mold rock textures. Therefore, distribution of knots determines the distribution of strokes. Notably, an exclusive region is involved to control the knot distribution and density.
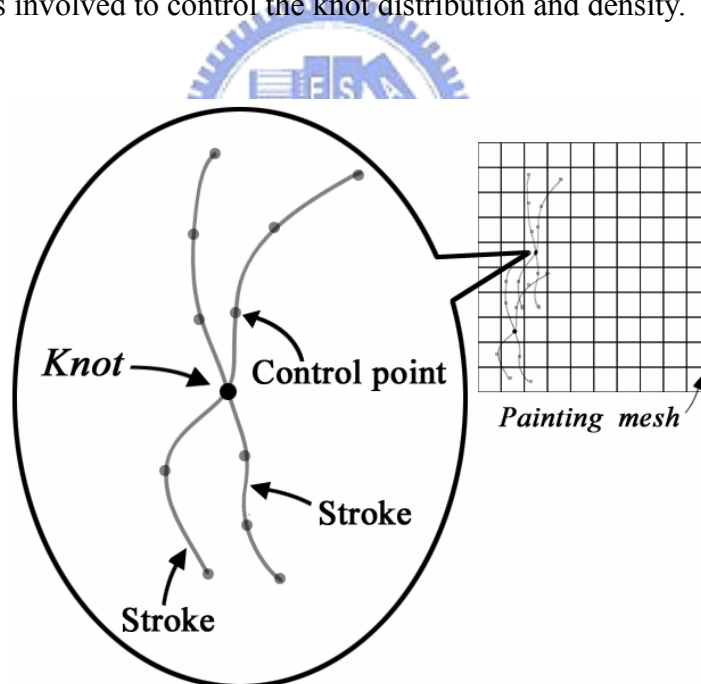

Figure 6.5: Two strokes generated by a knot.

6.3   Stroke Length

When *hemp-fiber* texture strokes are painted, long strokes present a continuous physiognomy of rock, and short strokes make the rocks appear rough and coarse. Since strokes are constrained in the 10×10-grid painting mesh, we limit the stroke length from 1 to 10. Under this mechanism, the length of a stroke refers to how many squares this stroke overstretches in Y direction of a painting mesh. Because we specify "which" square but not "where" to start or terminate a stroke, the actual lengths of strokes are similar, but not the same. Figure 6.6 shows strokes with different average lengths.
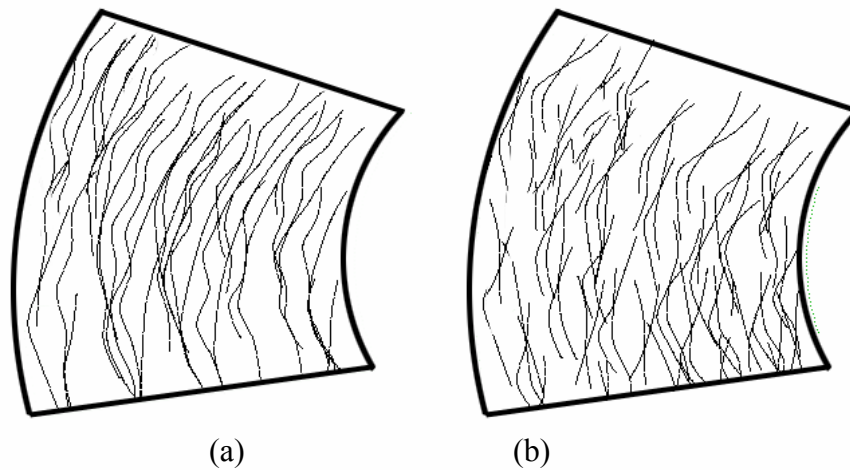

(a)   (b)

Figure 6.6: (a)Average length =8; (b)Average length =5.

6.4   Crossing Angle

A knot can generate two strokes, which cross each other at the knot, accounting for why the orientation of strokes can be controlled by crossing angles between these two strokes. In Chinese landscape painting, the orientation and intertwinement of rock strokes are essential.

Particularly in *hemp-fiber* strokes, strokes should follow some particular direction and intertwine with each other.
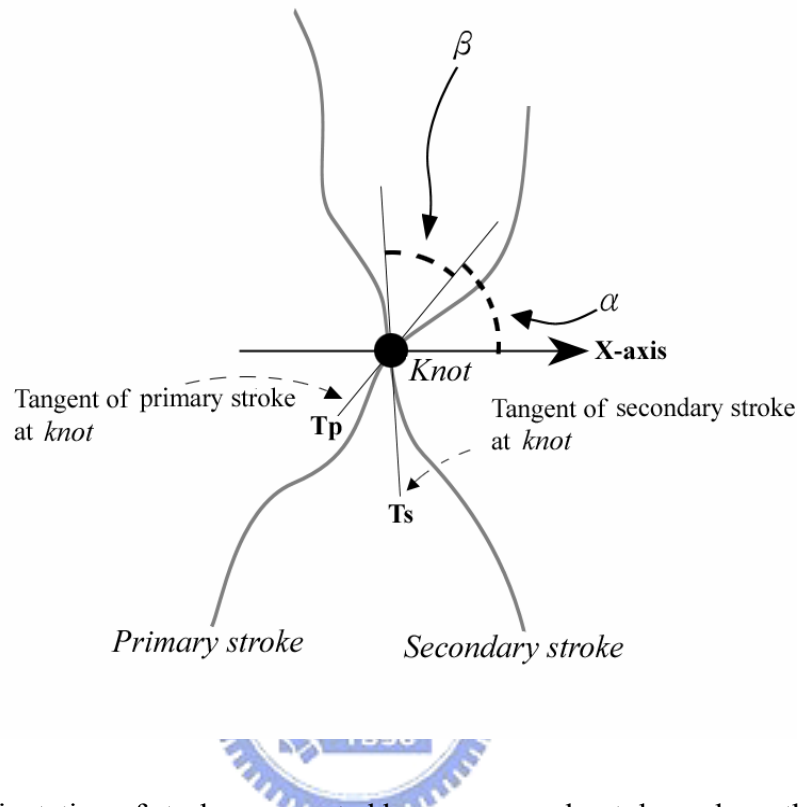

Figure 6.7: Orientation of strokes generated by a common knot depends on the α and β.

Consider Figure 6.7. Assume that a knot generates two strokes, the primary stroke and the secondary stroke. Where Tp and Ts denote the tangent of the primary stroke and secondary stroke at the knot, respectively. Herein, crossing angles are classified into two categories: α and β. Where α is between Tp and X-axis, and β is between Tp and Ts. When crossed strokes are generated at a knot, orientation of the primary stroke is determined according to α. Similarly, orientation of secondary stroke is determined according to β. Figure 6.8 shows different values of α and β, resulting in different orientations of strokes. Besides, β is used to control the stroke intertwinement.
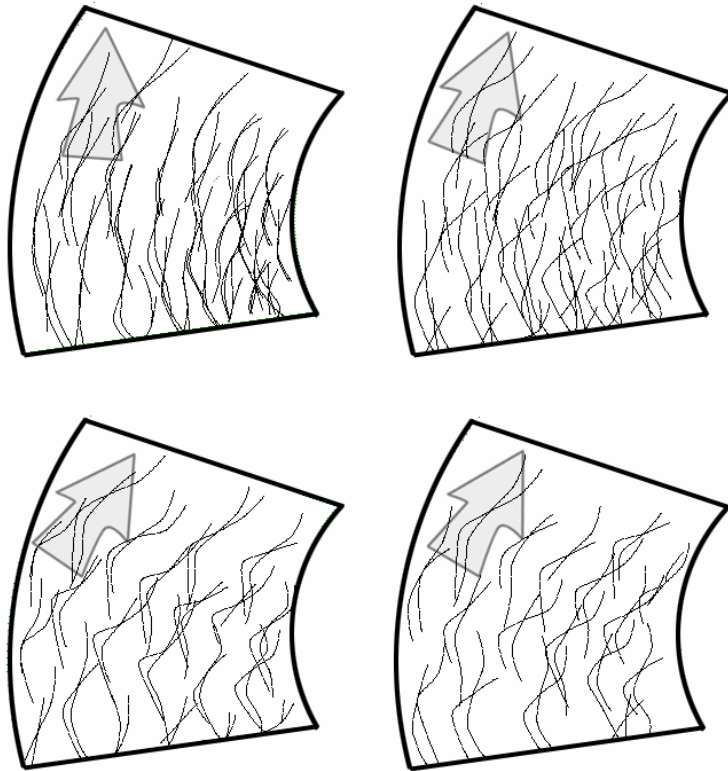
Figure 6.8: Strokes with different α and β.

6.5 Perturbation

Visually, slightly perturbed strokes make rock surfaces appear more undulating. For presenting various rock surfaces, stroke perturbation should be considered an important parameter. Owing to that the strokes are represented in Cardinal spline, the curve can be perturbed by moving the control points. For each stroke, a control point in each row is located, where this stroke overstretches in a painting mesh. These control points can be moved in a proper range. If perturbed strokes are applied, the moving range of each control point is amplified simultaneously. A large moving range implies that control points can not be controlled at a fixed location.

6.6 Experimental Results

Figure 6.9 illustrates the area surrounding the texture strokes and the corresponding painting meshes of an original painting by Huang Kung-wang shown in Figure 6.1. Figure 6.10 is the resulting image from Figure 6.1; Table 6.1 gives the brush parameters of Figure 6.10. Figure 6.11 shows the resulting image from Figure 6.2 with *axe-cut* texture strokes by our method.
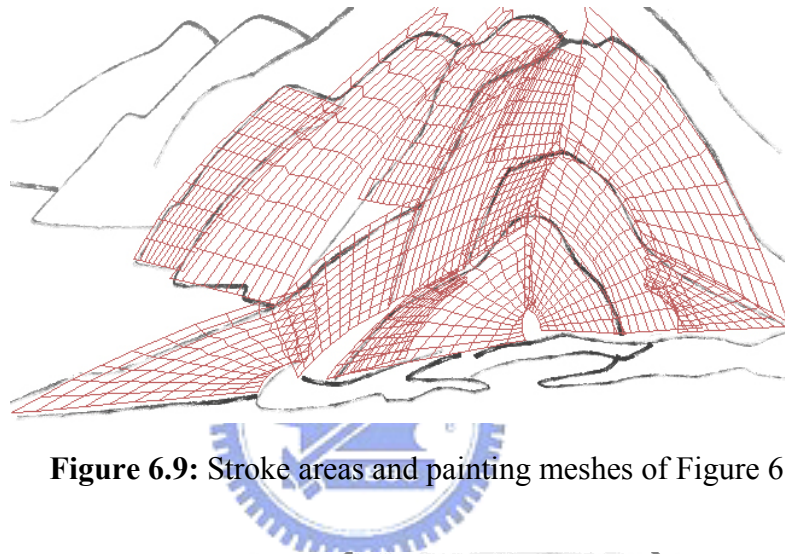

Figure 6.9: Stroke areas and painting meshes of Figure 6.1.

Figure 6.10: Resulting image of Figure 6.1 by our method.

Table 6.1: Stroke parameters of Figure 6.10

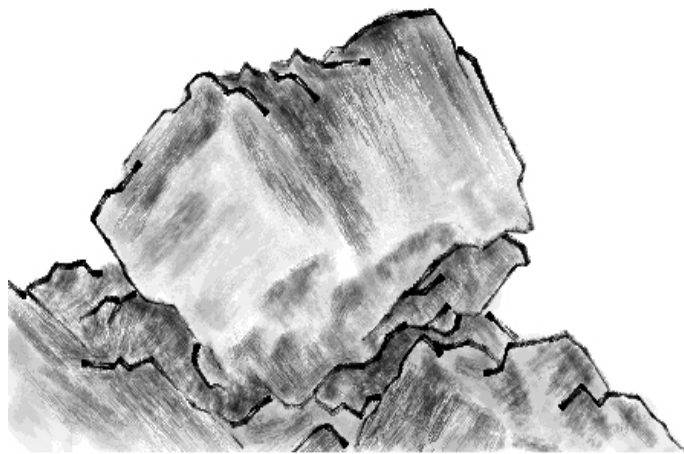| Number of painting mesh	Stroke's size	Turning point pressure	Cardinal spline (t)
18	2	0.4	0.2

Figure 6.11: Resulting images of Fig. 6.2 by our method.
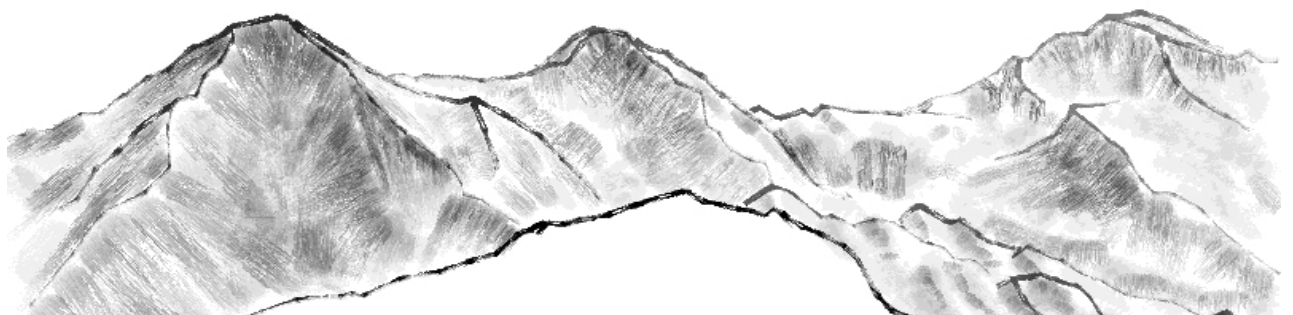

Figure 6.12: Jungfraujoch-Top of Europe.

Figure 6.13: Jungfraujoch-Top of Europe with axe-cut texture strokes.

Our methods may also depict a real scene into Chinese landscape painting. Figure 6.12 displays photographs of Jungfraujoch Mountain – "Top of Europe". Figure 6.13 illustrates corresponding ink paintings generated with *axe-cut* texture strokes by our method. Figure 6.14 shows the picture "Titlis Mountain", by Lin Yu-Shan who is a famous artist in Taiwan. Figure 6.15 summarizes those results of "Titlis Mountain" by our method. Finally, Figure 6.16 is a photograph of Lan-Yan River in Taiwan. Figure 6.17 shows the Lan-Yan River with *hemp-fiber* texture strokes.
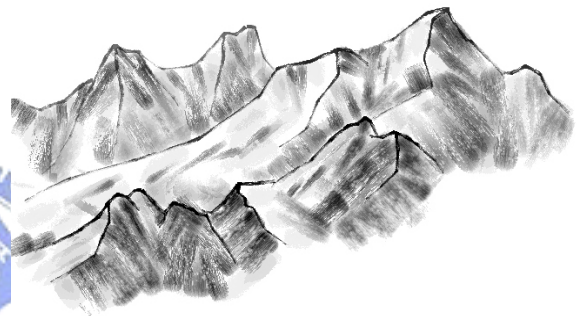

Figure 6.14: "Titlis Mountain", by Lin Yu-Shan. **;**

Figure 6.15: Imitate "Titlis Mountain".

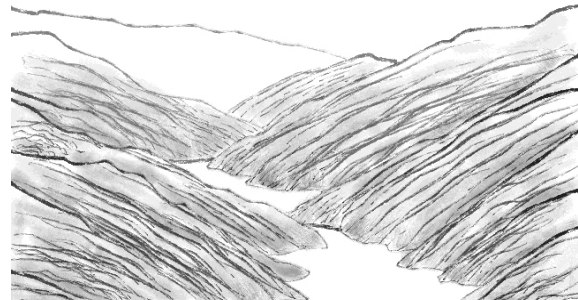**Figure 6.16:** Lan-Yan River in Taiwan**;**

Figure 6.17: Lan-Yan River with *hemp-fiber* strokes.

Chapter 7

Texture Strokes Construction with 3-Dimension Terrain

This chapter describes the rendering of texture strokes and the use of the traditional brush technique to create primitive strokes. Figure 1.1 illustrates the process of producing texture strokes, which includes several basic elements: First, 3D information is extracted to render the texture of the rock. Second, the outline of the silhouette is created. Third, the direction field on the surface is computed and the streamlines of texture strokes generated. Finally, brush strokes are applied to create an outline drawing and the rock texture captured with vertical or slanted strokes along the control lines with a rich ink tone specified by shading value. Users can easily choose a style of texture stroke and input parameters for controlling the desired effects. The proposed method then automatically completes the painting process.

7.1 Extracting 3D Information

The Digital Elevation Model (DEM), also known as a grid field, is a popular terrain file format in science and engineering applications. All the terrain models presented here were

provided by 3DEM Visualization Software [52]. Moreover, the grids of DEM heights were transformed into adjacent triangles. The inputs of the 3D terrain polygonal models were rendered using OpenGL include vertices, edges and faces. Moreover, the shading intensity was determined using the luminance map. The gray-scaled image specifies the ink tone values. All information can be extracted during the pre-process step without user intervention.

7.2 Drawing of Outlines

The outline, or silhouette, of a shape is a typically dominant feature. This research attempts to render attractive silhouette outlines for 3D geometry, creating brush-strokes along well-chosen paths around each object. The rending involves three distinct phases. First, the location of silhouette edges is determined. Second, links these silhouette edges into a long path. Third, each brush stroke is drawn in a style defined by the user.

The silhouette set for the smooth surface is the set of points P of the surface such that $(n(P) \cdot (P - C)) = 0$, where C is the viewpoint, $n(P)$ is the normal vector of P. The silhouette is a union of flat areas, curves and points on the surface. However, the silhouettes of smooth surfaces are significantly different from those of their approximating polygonal meshes. For polygonal meshes, if the viewing vector (V) is defined as a vector from the viewpoint (C) to the viewing plane, then a front facing polygon is identified by the sign of the dot product of N (the polygon normal $n(P)$) and V. If the dot product $N \cdot V > 0$, then the polygon is front-facing; if $N \cdot V < 0$, then the polygon is back-facing, and if $N \cdot V = 0$, then the polygon is perpendicular to the viewing direction.

A silhouette edge is defined as one that connects a front-facing triangle to a back-facing

triangle. The edge can also be a silhouette edge if it is not connected to another triangle. Then, visibility and adjacency are computed from a 2D projection of the silhouette edges. The next step links these silhouette edges into long chains, or paths, which will form the basis of the brush strokes. These silhouette edges must be computed whenever the view changes. These silhouette edges must be computed whenever the view changes. Figure 7.4(d) extracts the silhouette edge from Figure 7.4(a) and applies the vertical brush stroke.

7.3 Generation of Streamlines

A direction field on the surface should be chosen for streamline generation. A natural geometric candidate is the pair of principal curvature direction fields [6, 41]. Ohtake et al. [28] presented adaptive smoothing tangential direction fields on a polygonal surface. Ohtake's method effectively simulated pen-and-ink drawings of 3D objects. However, Chinese landscape painting seeks to simulate the surface texture of a terrain. The basic idea of generating streamlines is adjusted for applying texture strokes.

7.3.1 Streamlines

Given a triangulated surface and the principal curvature directions at each vertex, the weighted averaging scheme repeatedly and simultaneously updates each vertex direction by calculating the weighted sum of the directions. Selecting such a weight smooth the direction field and maintains the coherence of the reference direction. The reference direction is the gravity direction of the terrain. DEM is a grid field of height, so for any vertex P (P_x, P_y, P_z), P_y is the height of the vertex. Figure7.1 displays a triangular mesh F with normal vector $\vec{F}_n$.

Moreover, $\vec{G}$ denotes the direction of gravity (0,-1,0). Let $\vec{G}_{ref} = \vec{G} + \vec{F}_n$, where $\vec{G}_{ref}$ is the projection of vector $\vec{G}$ onto F. Finally, the vector $t(P)$ is the initial principal direction estimated at the vertices of the mesh $t(P) = (t(P) + \sum_{i=1}^{n}[Wi \times t(Q_i)])/(1 + \sum_{i=1}^{n}Wi)$, $Wi = (\overline{PO_i})/(\sum_{i=1}^{n}\overline{PO_i})$, where Q_i are all the neighboring vertices of P.
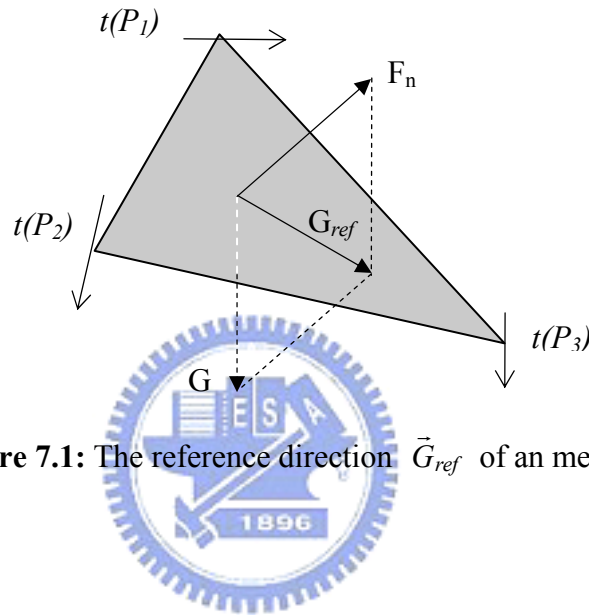

Figure 7.1: The reference direction $\vec{G}_{ref}$ of an mesh F.

The vector $t(F)$ is the streamline direction field combined with $t(P_1)$, $t(P_2)$, $t(P_3)$ and G_{ref} on triangle F, $t(F) = \alpha G_{ref} + (1-\alpha)(t(P_1)+t(P_2)+t(P_3))$, where $0 < \alpha < 1$. Restated, if a *raindrop* were to fall on surface F, it would flow along the streamline direction $t(F)$.

Once the streamline direction field is smoothed by the reference direction, a direction field $t(F)$ is defined on the face of every triangle mesh. An initial point inside a triangle is selected, and the streamline is traced from the point, according to $S_{k+1} = S_k + \rho t(F_k)$, where ρ is a real number such that the line meets the edge of the triangle. Moreover, S_{k+1} is located on the edge of the triangle. The tracing of the streamline ends when the streamline direction conflicts with another streamline direction of the neighboring triangle, as shown in Figure 7.2, where the streamline stops at a ravine. Each triangle mesh can generate one streamline.

Figure7.4(b) depicts the resulting stroke streamlines obtained by this method.

The segments of S_i are defined by *segment(S_i),* which is number of triangles through which S_i passes. For example, *segment(S)* is 9 in Figure 7.2. The average of *segment(S_i)* of a terrain is defined by $AVG\ (S) = (\sum_{i=1}^{n} [segment\ (S_i)]) / n$, where n denotes the number of triangular meshes of a terrain. Normally, the number of iterations required for smoothing is *AVG(S)*.
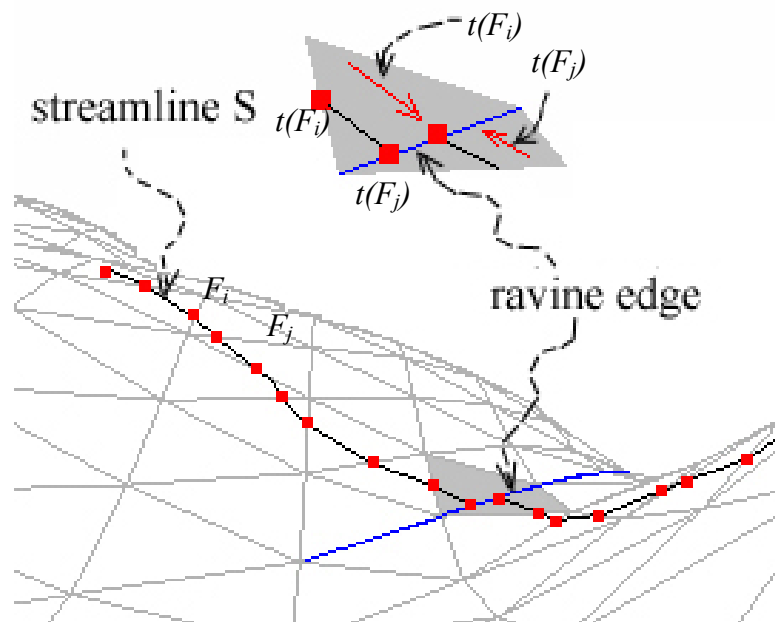

Figure 7.2: An example of streamlines generation

7.3.2 Ridge Mesh

The following steps are performed to determine whether a mesh F is a ridge mesh of a terrain model. (1) Locate all the streamlines; every triangle generates one streamline, which does not stop until it meets the ravine; (2) Compute the number of streamlines $S_{total}(F_i)$ that pass through the triangle mesh F_i; (3) specify a threshold $S_{threshold}$: if the number of streamlines

$S_{total}(F_i) \leq S_{threshold}$. Then, F_i is a ridge triangle mesh. Let *Ridge(F)* represent a set of triangle meshes, *Ridge(F)* = { $S_{total}(F_i) \leq S_{threshold}$; $0 \leq i < n$, where *n* is the number of triangle meshes of a terrain}. Normally, the mesh of the mountain peak only generates one passing streamline ($S_{total}(F_{peak}) \leq 1$). Figure7.3(c) plots the streamlines generated using ridge meshes. The ridge triangle mesh is extremely important for rendering *lotus-leaf* texture strokes.

7.3.3 Level of Detail

The level of detail (LOD) modeling method is an effective approach for interactively visualizing complex terrain models. When the terrain is so far away that it only occupies one pixel, there is very little use in modeling the terrain in high detail. Figure 7.3(a) plots all streamlines without LOD, the entire streamlines do not need to be displayed in significant detail because they may be obscured by a visible piece of the model, or be far enough away to make the detail meaningless. A large number of researchers have developed algorithms for approximating terrains and other height fields using polygonal meshes. Taylor and Barrett [40] extract mesh approximations from rectangular quad-tree hierarchies. Both Lindstrom et al. [22] and Duchaineau et al. [5] define binary-tree hierarchies based on binary subdivision of right isosceles triangles, and demonstrate real-time view-dependent LOD. In the proposed approach, the number of strokes to be shown is determined with the LOD. For each initial vertex P_i of streamline S_i, *Depth(P_i)* represents the depth value of P_i . Based on the *Depth(P_i)* value, look up the hierarchical tree which streamline S_i is selected or not. The streamlines are completely visible only when close to the viewer. Figure7.3(b) depicts the stroke streamlines using LOD. LOD is creating an impression of viewing distance when rendering terrain. The depth value also influences the width of the streamline brush stroke.
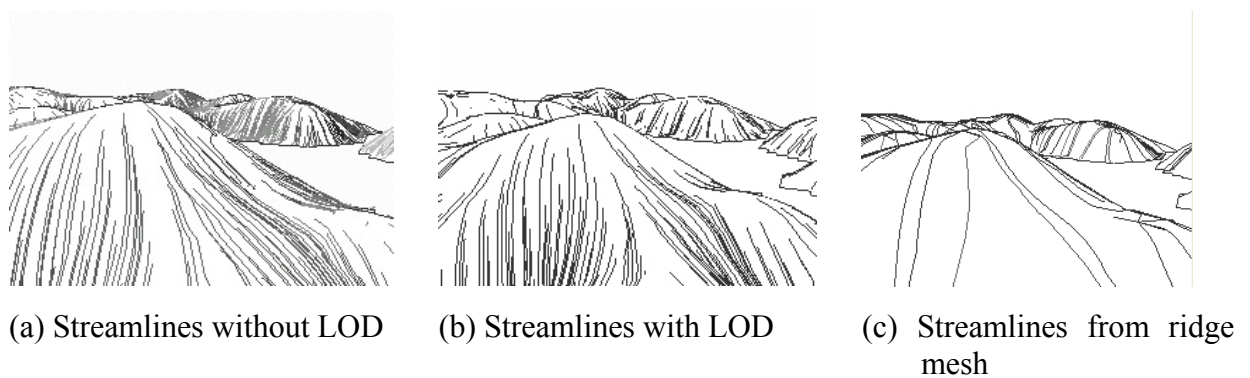
(a) Streamlines without LOD (b) Streamlines with LOD (c) Streamlines from ridge mesh

Figure 7.3: Examples of streamlines rendering with three different conditions

## 7.3.4 Brush Stroke of Streamlines

In order to generate brush strokes on the rice paper, the models of the previous work are utilized [39, 45, 46]. In this section, only explain the brush strokes of streamlines briefly.

The stroke of streamline is applied using a precise and flexible Cardinal spline. Cardinal spline is an interpolated but not approximated curve, which passes through all the specified control points. All points of one streamline can be selected as control points. Cardinal spline facilitates slackness control by adjusting parameter t, with a smaller t implying a slacker curve. Figure 5.5 illustrates the precision and flexibility of the Cardinal spline. The brush stroke line can be either softened or hardened.

7.3.5 Frame Coherence

Frame coherence is an important issue in NPR related research. If stroke placement and style differ significantly between two consecutive frames, coherency problems will result. Since streamlines are constructed during a preprocess step, the position of each streamline is fixed. Furthermore, stroke parameters such as the size of the brush, the number of bristles, the

decreasing rate of ink, water, and so on, are preserved. When strokes are applied at each frame, each stroke is guaranteed to have the same position and stroke parameters.
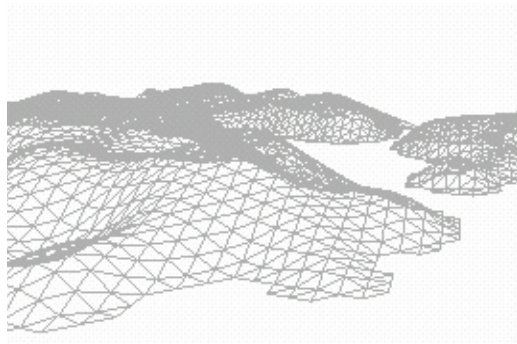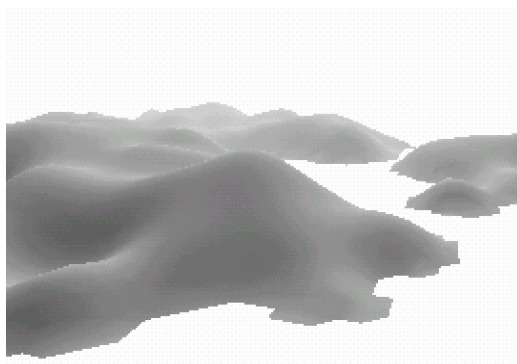

(a) Wireframe

(d) Outline drawing

(b) *Hemp-fiber* stroke streamlines

(e) *Hemp-fiber* texture strokes

(c) Smooth shading with fog

(f) *Hemp-fiber* texture strokes

Figure 7.4: The procedure of *Hemp-fiber* texture strokes

7.4 Interactive Texture Rendering

This work has designed an interactive application base on the surface wrinkle rendering diagram (Figure 1.1). This system has two editing modes: brush model and texture rendering. In each case, we provide an interface for direct user control, and rendering algorithms to support the required interactivity.

Our previous work provided a brush model that enables a user to paint the Chinese brush simulation with initial conditions. There are slider controls to adjust the physical parameters for the brush (ink decreasing, ink soaking variation, bristle material, bristle dry-out, wet effect, and ink blending). The details of brush model are described in [39, 45, 46]. The luminance map is a reference shading image for ink tone during ink diffusion.

When loading the terrain model, there are many 3D information need to extract before texture rendering (described in Section 7.1). Furthermore, the user selects one of the six texture styles and input parameters to control the desired effect (described in Section 5.2). Users can to adjust stroke length, width, density, and level of detail (LOD) through the conventional user interface. The proposed method then automatically completes the painting process. When the system renders the scene from a new perspective, it adapts the number and placement of the texture strokes as appropriate to maintain the textural consistency of the terrain.

7.4.1 Main Procedure

The main simulation procedure involves two phases: 3D information extraction and texture rendering. When loading the terrain model, the first significant task *FindNeighbor()* is determining the neighborhood relation of the faces and vertices. Based on the proposed methods described in section 1.2, *PrincipalCurvature()* computes the pair of principal curvature direction fields, *GenerateStreamLines()* generates the streamline for each triangular mesh, *FindRidge()* identifies the all ridge meshes and *CreateLODtree()* establishes the hierarchical tree for the level of detail. During the texture rendering phase the user selects a texture style and input parameters for controlling the desired effect.

```
Proc Extract3DInformation(Terrainfilename)
FindNeighbor();          // find the neighborhood relation of the face and vertex.
PrincipalCurvature();    // calculate the pair of principal curvature direction fields.
GenerateStreamLines();   // generate streamline for each triangular mesh.
FindRidge();             // find the all ridge meshes.
CreateLODtree();         //create the hierarchical tree for the level of detail.
end Proc


Proc TextureRendering( )
   switch (Rendeing_Type)
   {
      case HEMP_FIBER: HempFiberStroke();
      case AXE_CUT:    AxeCutStroke();
      case LOTUS_LEAF: LotusLeafStroke();
      case RAIN_DROP:   RainDropStroke();
      case MI_DOT:      MiDotStroke();
      case BONELESS:       BonelessStroke();
   }
   end Proc
```
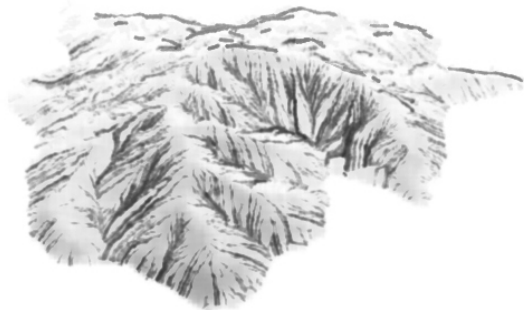
7.4.2 Six Rendering Styles

Hemp-Fiber Stroke

Streamlines can be generated using the above method for representing various rock surfaces. When *hemp-fiber* texture strokes are applied, each streamline is projected onto a 2D viewing plane and represented using the Cardinal spline to form one stroke path. If the streamline is visible and selected by LOD (*w>0*), then paint it using vertical brush stroke with width *w*. To create a natural effect, stroke perturbation should be considered as another parameter by moving the control points. Figure 7.5(b) illustrates Angel Island in San Francisco Bay as represented using *hemp-fiber* strokes.

```
Proc HempFiberStroke()
for each streamline S[i]
{
w=LODtree(S[i]);        //w is the width of stroke
if (w>0 and S[i] is Visible)     BrushStroke(CardinalSpline(S[i]), Vertical, w);
}
end Proc
```
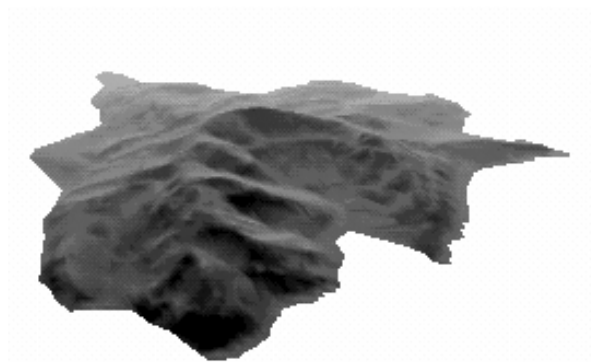

(a) Angel Island. (polygonal model)   (b) *Hemp-fiber* Stroke.

Figure 7.5: Examples of *Hemp-fiber* strokes in shaded area.

Lotus-Leaf Stroke

To draw the *lotus-leaf* stroke, this study only selected the streamlines that were generated by a ridge triangle mesh. The edge of the ridge forms the veins of the lotus leaf. The other steps are same as for a *hemp-fiber* stroke. Figure 7.6(a) illustrates Mount Olympus, Washington, and Figure 7.6(b) illustrates the simulated result obtained by applying *lotus-leaf* texture strokes.

```
Proc LotusLeafStroke ()
for each streamline S[i]
{
w=LODtree(S[i]); //w is the width of the stroke
if (w>0 and S[i] is Visible and S[i] is Ridge)
//using vertical stroke
BrushStroke(CardinalSpline(S[i]), Vertical, w);
}
end Proc
```
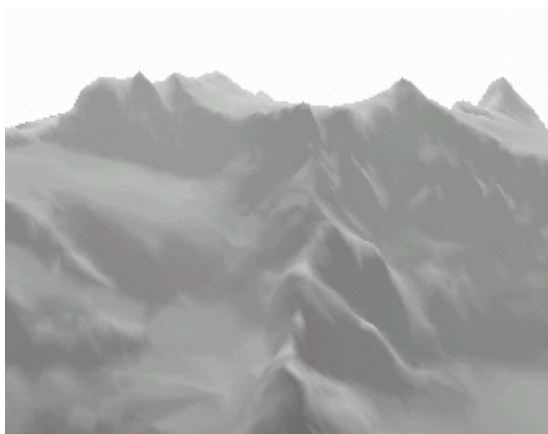

(a): Mount Olympus, USA. (polygonal model)   (b): *Lotus-leaf* Stroke.

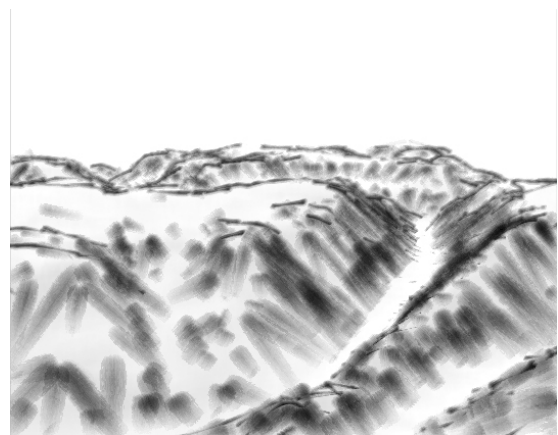**Figure 7.6:** Examples of *Lotus-leaf* strokes in shaded area.

Axe-Cut Stroke

The *axe-cut* stroke is a slanted stroke. An artist slants the brush so that the brush tip bends slightly sideways. Normally, the stroke has a rectangular or triangular shape. The process of applying an *axe-cut* texture stroke is the same as for applying the *hemp-fiber* stroke. The only difference is the application of the slanted brush stroke along the streamlines. Figure 7.7(b) illustrates the Grand Canyon as represented using *axe-cut* strokes.

```
Proc AxeCutStroke ()
for each streamline S[i]
{
w=LODtree(S[i]); //w is the width of the stroke
if (w>0 and S[i] is Visible)
//using the slanted stroke
BrushStroke(CardinalSpline(S[i]), Slanted, w);
}
end Proc
```
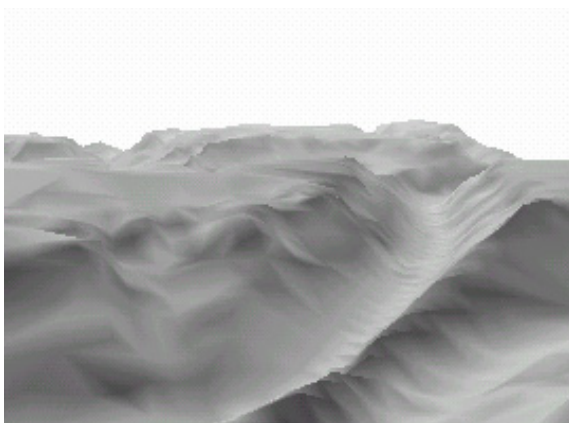

(a): the Grand Canyon. (polygonal model)   (b): *Axe-cut* Stroke.

Figure 7.7: Examples of *Axe-cut* strokes in shaded area.

Raindrop Stroke and Mi-Dot Stroke

The dot texture strokes use the vertex of a streamline to replace an edge. The position of the vertex is perturbed to create a natural effect. The dot size depends on the depth value and a random number. Figure 7.8(a) plots the model of a mountain and Figure 7.8(b) depicts the *raindrop* dot formed using a wet brush. The Mi dots are applied using the vertex of the streamline of a *lotus-leaf* and a ridge vertex. A horizontal line then is created at each vertex. The length of each horizontal line also depends on the depth value and the distance from the top ridge. Figure7.8(c) displays the simulated result obtained using a wet brush.

Proc RainDropStroke ()
for each streamline S[i]
{
w=LODtree(S[i]); //w is the the stroke width
if (w>0 and S[i] is Visible) PaintDot(S[i], w);
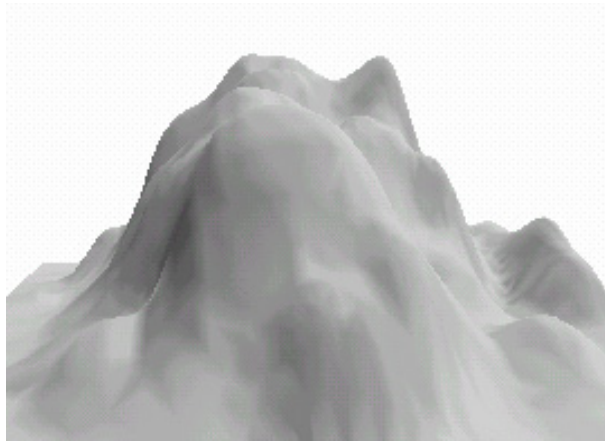*}*
end Proc

Proc MiDotStroke ()
for each streamline S[i]
{
w=LODtree(S[i]); //w is the width of the stroke
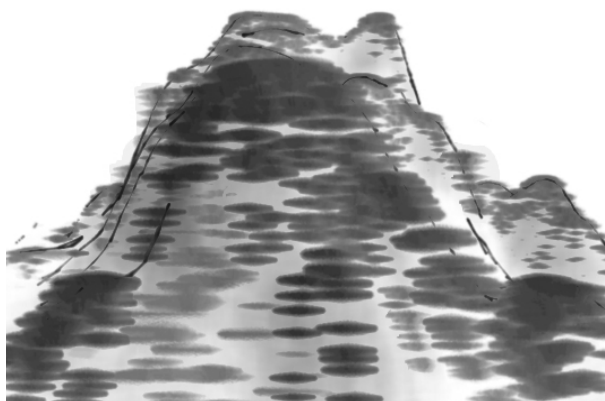*if (w>0 and S[i] is Visible and S[i] is Ridge) PaintMiDot(S[i], w);*
}
end Proc

(a) Mountain (polygonal model)

(b) *Raindrop* Stroke

(c) Mi dots Stroke

Figure 7.8 : Examples of *Raindrop* and *Mi-Dot* strokes in shaded area.

Boneless Stroke

As described in section 3, in a *boneless* stroke, the ink is dark close to the edge of the silhouette, and lightens with increasing distance from the edge. The proposed method for representing the ink-gradient of a *boneless* stroke in manual painting is as follows. First, the edges of the silhouette are determined. Second, the distance between a pixel and silhouette pixel must be calculated. Third, a brush stroke with an ink tone dictated by distance is applied. Finally, the ink is diffused by the very wet brush.

| (a) | (b) |
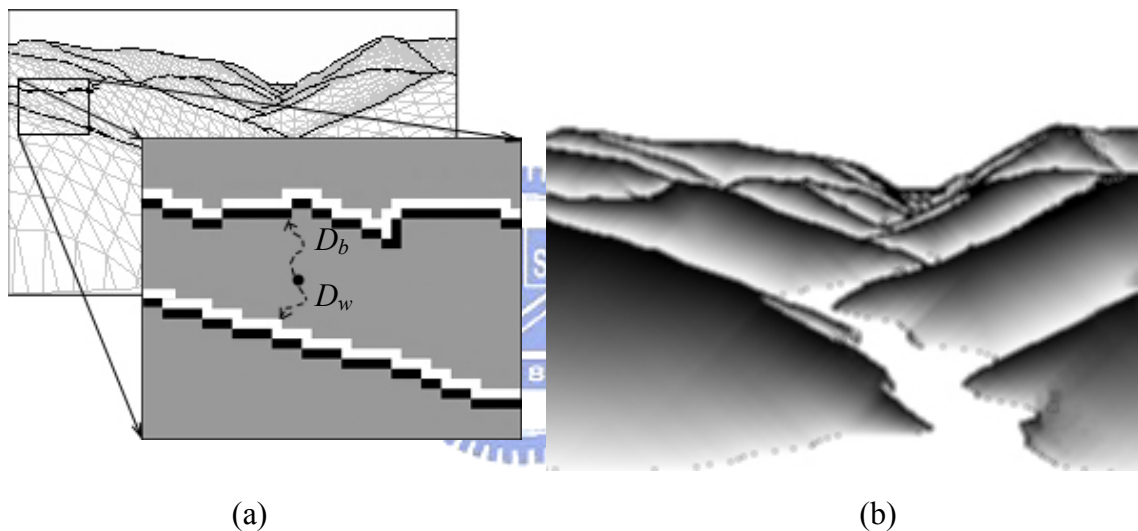
Figure 7.9: An example of distance value between silhouette and boundary.

In this work, silhouette edges are determined in a 3D object-space. However, the distance from each pixel to the silhouette is determined in a 2D image space. Figure 7.9(a) illustrates black silhouette lines. The color of the neighbor pixel of the silhouette is white if the neighbor pixel is not projected from the face of the same triangle or the neighboring triangle. Restated, the white pixel is a boundary pixel. Moreover, D_b is the minimum distance from a pixel to the silhouette, and D_w is the minimum distance from a pixel to the boundary, as shown in Figure 7.9(a). To normalize the distance from zero to one, let $D = D_b / (D_b + D_w)$. Figure 7.9(b)

displays the initial ink tone determined based on the distance value. Finally, the ink diffuses in a manner determined by the distance value and foggy luminance map. Figure 7.10(a) depicts a terrain model and Figure 7.10 (b) illustrates the result of Fig 7.10 (a) for *boneless* strokes.
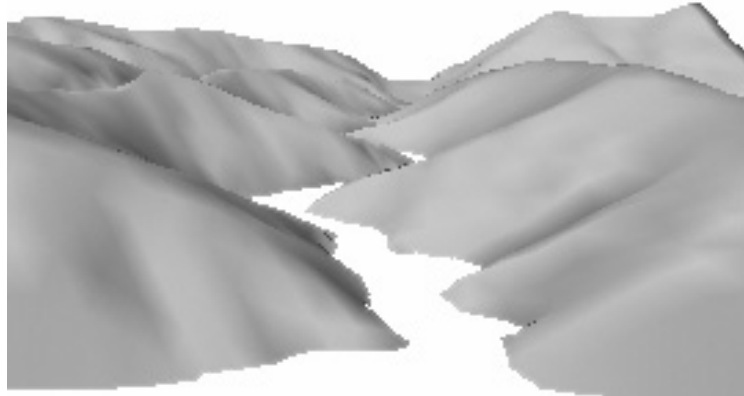
(a) 3D polygonal model
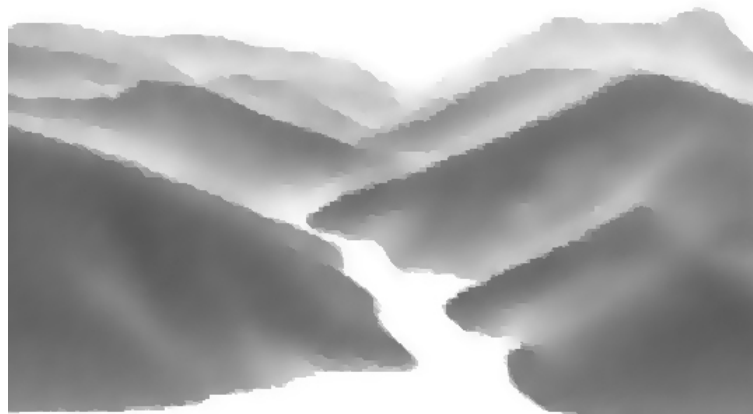
(b) *Boneless* stroke

Figure 7.10: An example of the *boneless* stroke by our method.

7.5 Experimental Results

Table 7.1 lists the performance measurements of the proposed methods. The first column refers to the figures, and the second column contains the number of all of the polygons in a scene. Finally, the third column indicates the user specified surface wrinkle type. The fourth column reflects the computation time of streamlines generation when the terrain is loaded. The fifth and sixth column shows the rendering time under different conditions. The final two columns display the painting time for two image sizes. The computational time of ink painting depends on the number of visible streamlines to be drawn and the image size. Figure 7.11 and 7.12 show the result using numerous wrinkles. Figure7.12 (c) integrates wrinkles with tree-dots and water wave lines. Figure 7.13 displays Angel Island as rendered in *hemp-fiber* strokes from various viewpoints.

Table 7.1: Performance measurements (sec)

	Number of Polygons	Surface Wrinkle	Streamlines			Ink Painting	
			Generation	Rendering (1)	Rendering (2)	270x225	540x450
Figure 7.5	7,946	hemp-fiber	3.856	0.104	0.085	5.791	11.806
Figure 7.6	8,391	lotus-leaf	4.238	0.168	0.065	3.754	6.211
Figure 7.7	7,317	axe-cut	2.385	0.089	0.070	6.499	10.021
Figure 7.8 (b)	7,118	raindrop	3.695	0.098	0.096	3.189	7.801
Figure 7.8 (c)	7,118	Mi-dot	3.695	0.086	0.049	5.644	9.628
Figure 7.10	5,408	boneless	1.205	0.083	0.018	1.389	5.711
Figure7.11 (b)	17,461	hemp-fiber, lotus-leaf, axe-cut and boneless.	7.175	0.213	0.137	6.749	14.305
Figure 7.12(b)	14,703	hemp-fiber , outline and boneless	6.118	0.209	0.108	3.561	9.065

(1) Rendering all streamlines without LOD;
(2) Rendering the streamlines of user's specified wrinkles with LOD.

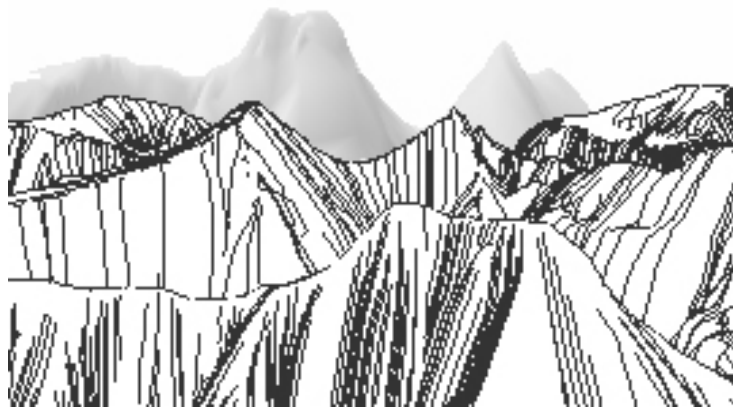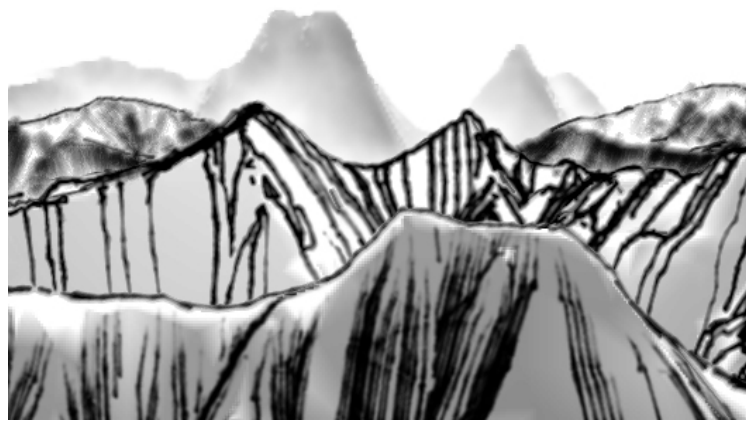**Figure 7.11(a) :** Streamlines.

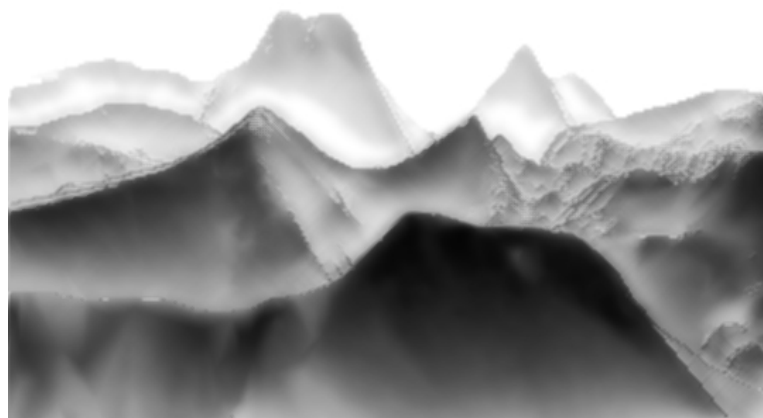**Figure 7.11 (b) :** *Hemp-fiber*, *lotus-leaf*, *axe-cut* and *boneless*.

Figure 7.11 (c) : *Boneless* Stroke

Figure 7.12 (a) : Streamlines.

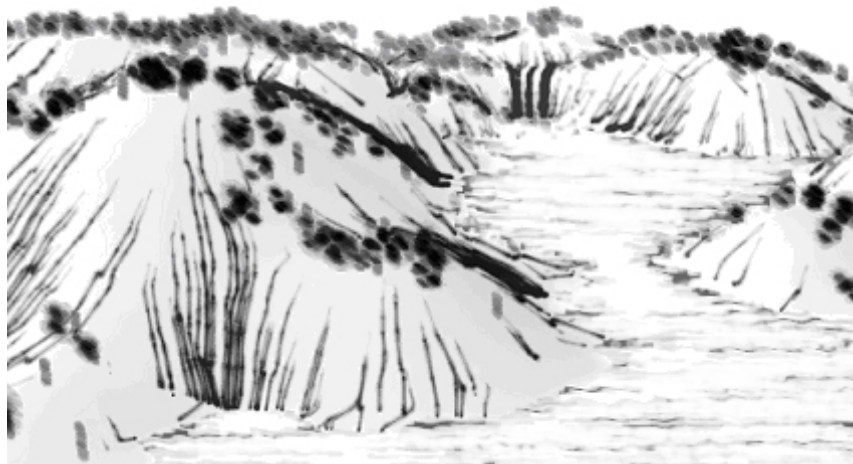**Figure 7.12 (b) :** *Hemp-fiber*, outline and *boneless*.

Figure 7.12 (c) : *Hemp-fiber*, tree-dots and water's wave line.
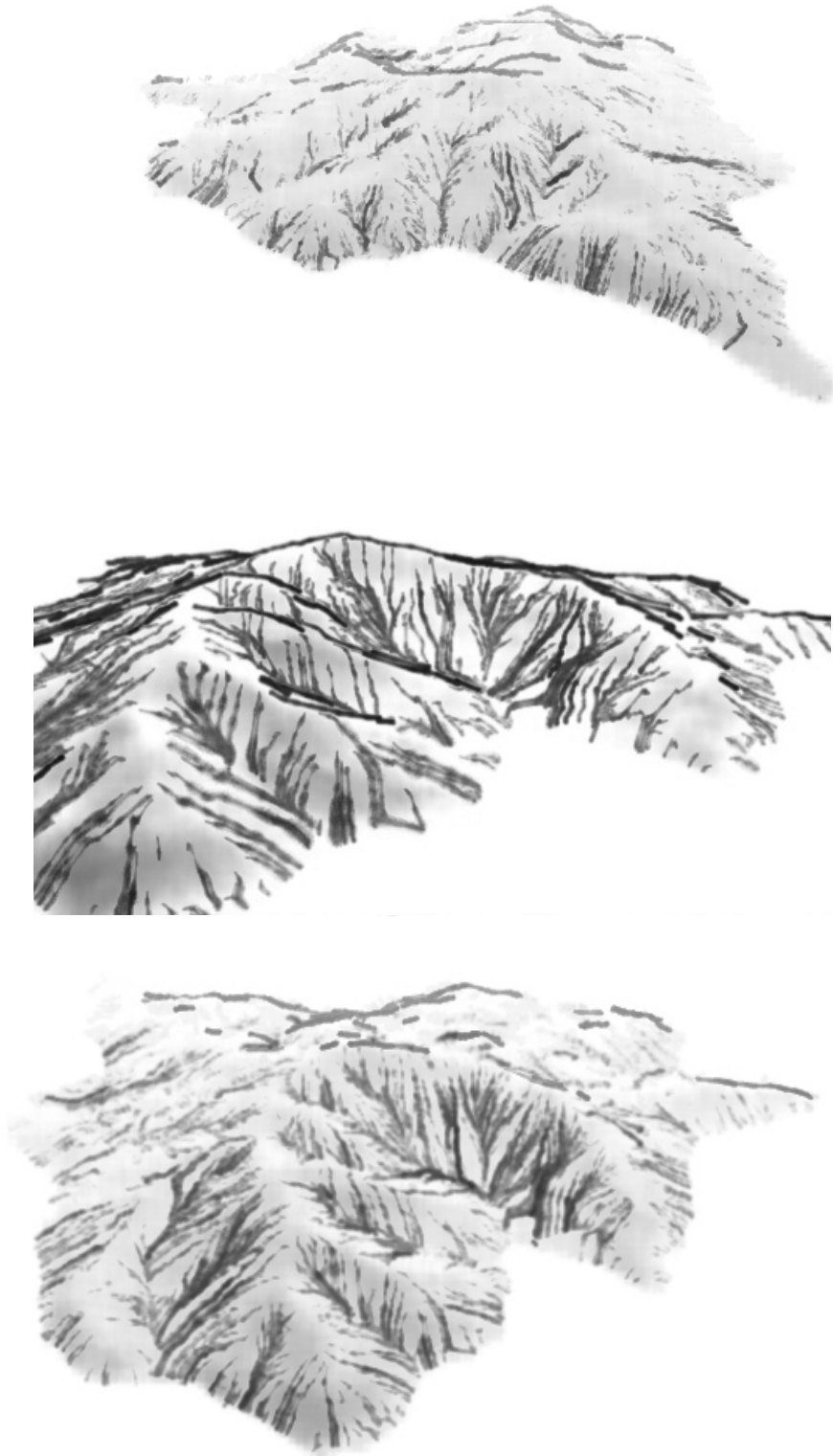
Figure 7.13: *Hemp-fiber* stroke of Angel Island in different viewpoint.

Chapter 8

Conclusion and Future Works

Computer graphics-related research has focused on obtaining photorealistic images since 30 years ago. Today, it is easy and powerful to construct a photo-realistic virtual world through many developed methods and graphic accelerator. However, photorealism is occasionally not the most effective means of visually expressing emotions. Accordingly, photographs can never entirely replace paintings. Non-photorealistic rendering (NPR) approaches have recently received renewed interest. In recently years, most research in NPR focused on Western painting. Many researches have addressed Western painting, including watercolors, impressionistic painting, pencil sketches and hatching strokes. Recent research on non-photorealistic rendering has focused on modeling traditional artistic media and styles including pen-and-ink illustration and watercolor painting…etc. These methods deliver good results for Western painting. But these approaches are not appropriate to Chinese ink painting. To simulate the style of Chinese ink painting is not trivial at all. It usually uses brushes and ink as mediums, values the expression of the artistic conception far beyond the precise appearance of the painted subjects. By means of the blending effects of brushes and ink, a painter communicates their frame of mind to the viewers.

Landscapes are one of the most important themes in Chinese painting. It is a form of non-photorealistic rendering. A painted of Chinese landscapes must understand both texture strokes and ink brush techniques. In Chinese landscape painting, rock textures convey the orientation of mountains and contribute to the atmosphere. Several landscape-painting skills are required to capture various types of rock. This thesis presents a set of novel methods for rendering rock textures in Chinese landscape painting. A 3D rock is drawn as an outline and texture strokes, using information on the shape, shade and orientation of the rock's polygonal surface. This work also uses vertical or slanted brush strokes for drawing outlines and rock textures. The main contribution of this work is on the modeling and implementation of an integrated framework for rock texture rendering using traditional brush techniques in Chinese landscape painting. The proposed rendering technique involves three major works.

1. This thesis presents a new method for simulating ink diffusion based on observation and analysis. The proposed method can simulate various expressions of tones on different types of paper. The elucidation of the effect of mixing simulated strokes made by different kinds of brushes is an important contribution of the method.

2. This thesis also provides a novel method of synthesizing rock textures in Chinese landscape painting on 2D image space, useful not only to artists who want to paint interactively, but also in automated rendering of natural scenes. The method proposed underwrites the complete painting process after users have specified only the contour and parameters.

3. Users can easily choose a style of texture strokes and input some parameters to control the desired effects. The proposed method underwrites the complete painting process automatically. The proposed rendering technique involves many parts: 3D information extraction; control line construction; projection onto a 2D image; brush stroke

application and ink diffusion. Effective results were also generated using the methods presented here.

Future studies should address the following issues to build upon the ideas presented here.

1. This work focuses on six main texture strokes. Although these are the most common texture strokes in Chinese landscape painting, many others should be developed. Developing other strokes would not be difficult since the concept of texture strokes closely resembles these six strokes.

2. Normally, Chinese landscape painting contains numerous objects, for example trees, rivers, lakes, clouds, boats, houses, and so on. Integrating with above objects is an interesting and important task.

3. A few recent studies have addressed real-time rendering. To date, ink diffusion remains a time consuming work. How to render ink diffusion with real-time will be a major future challenge.

Bibliograph

[1] C. C. Chiu and C. C. Ying, "Chinese Painting: A Comprehensive Guide", Art Book Co., Ltd., 1997.

[2] S. H. Chu and C. L. Tai. Real-time painting with an expressive virtual Chinese brush, IEEE Computer Graphics and Applications, Vol. 24, No.5, pp76-85,   2004.

[3] C. J. Curtis, S. D. Anderson, J. E. Seims, K. W. Fleischer, and D. H. Salesin, "Computer-Generated Watercolor", Proc.   SIGGRAPH 97, pp. 421-430. 1997.

[4] D. DeCarlo, A. Finkelstein, S. Rusinkiewicz, A. Santella. "Suggestive Contours for Conveying Shape", Proc. SIGGRAPH 2003, pp. 848-855.

[5] M. Duchaineau, M. Wolinsky, D. Sigeti, M. Miller, C. Aldrich and M. Mineev-Weinstein, "ROAMing terrain: real-time optimally adapting meshes", Proc. Visualization '97, IEEE, pp. 81–88, 1997.

[6] G. Elberg, "Interactive line art rendering of freeform surfaces", Computer Graphics Forum, Vol. 18, No. 3, pp. 1–12, 1999.

[7] B. Freudenberg, "Real-time stroke textures" (Technical Sketch) SIGGRAPH 2001 Conference Abstracts and Applications, p. 252, 2001

[8] L. M. Gao, "Chinese Painting by Chang Da-Chien", Art Book Co., Ltd. , 1988

[9] Q. Guo, "Generating Realistic Calligraphy Words," IEICE Transactions on Fundamentals of Electronics Communications and Computer Sciences, E78A(11):1556-1558, November 1996.

[10] Q. Guo, Tosiyasu L. Kunii, "Modeling the Diffuse Paintings of 'Sumie'". In: Kunii T (Ed.), Modeling in Computer Graphics (Proceedings of the IFIP WG5.10). Berlin: Springer, 1991. Page 329~338.

[11] A. Hertzmann, "Painterly Rendering with Curved Brush Strokes of Multiple Sizes", Proc. SIGGRAPH 98, pp. 453-460, 1998.

[12] A. Hertzmann and D. Zorin, "Illustrating smooth surfaces." Proc. SIGGRAPH 2000, pp. 517-526, 2000.

[13] A. Hertzmann,. "A survey of stroke-based rendering", IEEE Computer Graphics and

Applications, Vol. 3, No. 4, pp.70- 81, 2003

[14] S. W. Huang, D. L. Way, Z. C. Shih, "Physical-based model of ink diffusion in Chinese paintings", Journal of WSCG, Vol. 10, No. 3, pp.520-527, 2003.

[15] T. Isenberg, N. Halper, and T. Strothotte, "Stylized Silhouettes at Interactive Rates: From Silhouette Edges to Silhouette Strokes," Computer Graphics Forum, Vol.21, No. 3, pp. 249-258, 2002.

[16] Robert D. Kalnins, Lee Markosian, Barbara J. Meier, Michael A. Kowalski, Joseph C. Lee, Philip L. Davidson, Matthew Webb John F. Hughes Adam Finkelstein, "WYSIWYG NPR: Drawing Strokes Directly on 3D Models", Proc. SIGGRAPH 2002, pp. 755-762, 2002.

[17] A. Lake, C. Marshall, M Harris, and M. Blackstein, "Stylized rendering techniques for scalable real-time 3D animation." Proc. of NPAR2000, pp.13–20, 2000.

[18] J. Lansdown, S. Schofield, "Expressive Rendering: A Review of Nonphotorealistic Techniques," IEEE Computer Graphics and Applications, May 1995.

[19] J. Lee, "Simulating oriental black-ink painting", IEEE Computer Graphics & Applications 1999; 19(3): pp.74-81.

[20] J. Lee, "Diffusion rendering of black ink paintings using new paper and ink models", Computer & Graphics, Vol. 25, pp. 295-308, 2001.

[21] P. L. Lesage and M. Visvalingam, "Towards sketch-based exploration of terrain", Computers & Graphics 26 (2), pp. 309 - 328. 2002

[22] P. Lindstrom, D. Koller, W. Ribarsky, L. Hodges, N Faust, and G. Turner, "Real-time, continuous level of detail rendering of height fields", Proc. SIGGRAPH '96, pp. 109-118, 1996.

[23] P. Litwinowicz, "Processing images and video for an impressionist effect," Proc. SIGGRAPH 97, pp. 407-414, 1997.

[24] Y. Liu, "Ten thousand mountains, Shui-Yun-Chai Studio", pages 56–73 East Hampton Boulevard, Bayside, New York 11364, 1984

[25] L. Markosian, M. A. Kowalski, S.J. Trychin, L.D Bourdev, D. Goldstein, and J. F. Hughes, "Real-time nonphotorealistic rendering", Proc. of SIGGRAPH 97, pp. 415-420, 1997.

[26] M. Masuch, S. Schlechtweg, B. Freudenber, "Animating Frame-to-Frame Coherent Line

Drawings for Illustrative purposes ," Uinversitätsplatz 2, D-39106 Magdeburg, Germany.

[27] B. J. Meier, "Painterly Rendering for Animation," Proceedings of ACM SIGGRAPH 96, page 477-484, 1996.

[28] Y. Ohtake, M. Horikawa, A. Belyaev. "Adative smoothing tangential direction fields on polygonal surfaces". IEEE Computer Graphics and Application, 2001 Proceedings of 9th Pacific Conference. pp. 189-197, 2001

[29] E. Praun, H. Hoppe, M. Webb, and Finkelstein, "A real-time hatching", Proc. SIGGRAPH 2001, pp. 579-584, 2001.

[30] C. Rössl, L. Kobbelt and H. Seidel, "Line art rendering of triangulated surfaces using discrete lines of curvature", Proc. WSCG 2000, pp. 168-175, 2000.

[31] C. Rössl and L. Kobbelt. "Line art rendering of 3D-models". Proc. Pacific Graphics 2000, pp. 87-96, Los Alamitos, 2000. IEEE Computer Society Press.

[32] C. Rössl and L. Kobbelt. "Approximation and visualization of discrete curvature on triangulated surfaces", Proc. VMV 99, pp.339-346, 1999.

[33] S. Saito and M. Nakajima, "3D physics-based brush model for painting", Proc. SIGGRAPH 99:conference abstracts and applications, Page 226, 1999.

[34] Y. Sato, T. Fujimoto, K. Muraoka, N. Chiba, "Storoke-based Suibokuga-Like Rendering for Three-Dimensional Geometric Models - Ten and Shun Touches ", The Journal of the Society for Art and Science, Vol 3, No.4, pp. 224-234, 2004

[35] M. P. Salisbury, M. T. Wong, J. F. Hughes and D. H. Salesin, "Orientable textures for image-based pen-and-ink illustration", Proc. SIGGRAPH 97, pp. 401-406, 1997.

[36] D. L. Small, "Simulating Watercolor by Modeling Diffusion , Pigment and Paper Fibers", SPIE Proceedings, Vol. 1460, No. 15. San Jose, CA, 1990.

[37] M. C. Sousa and J. W. Buchanan, "Observational model of blenders and erasers in computer-generated pencil rendering", Proc. Graphics Interface '99, pp.157-166, 1999

[38] M. C. Sousa and J. W. Buchanan, "Computer-generated graphite pencil rendering of 3D polygonal models", Computer Graphics Forum, Vol. 18, No. 3, pp.195-208, 1999.

[39] S. Strassmann, "Hairy brushes" , Proc. SIGGRAPH 86, pp. 225-232. 1986.

[40] D. C. Taylor and W. A. Barrett, "An algorithm for continuous resolution polygonalizations of a discrete surface". Proc. Graphics Interface '94, pp. 33–42, 1994.

[41] L. Victoria, "Interrante illustrating surface shape in volume data via principal direction-driven 3D line integral convolution", Proc. SIGGRAPH 97, pp. 109-116, 1997.

[42] M. Visvalingam and K. Dowson, "Towards cognitive evaluation of computer-drawn sketches", The Visual Computer 17 (4), pp. 219-235.

[43] M. Visvalingam and J. C. Whelan, "Occluding contours within artistic sketches of terrain", Proc. 16th Conference of Eurographics-UK, pp. 281-289, March 1998

[44] M. Visvalingam, K. Dowson, "Algorithms for Sketching Surfaces," Computer & Graphics, Vol. 22, No 2-3, page 269-280, 1998.

[45] D. L. Way, Z. C. Shih, "The synthesis of rock textures in Chinese landscape painting", Computer Graphics Forum, Vol. 20, No. 3, pp. C123-C131, 2001.

[46] D. L. Way, Y. R. Lin, Z. C. Shih, "The synthesis of trees in Chinese landscape painting using silhouette and texture strokes", Journal of WSCG, Vol. 10, No. 3, pp. 499-507, 2002.

[47] Helena T. F. Wong, Horace H. S. IP, "Virtual Brush: a Model-based Synpaper of Chinese Calliigraphy,' Computer & Graphics, Vol 24 , 99-113, 2000.

[48] G. Winkenbach and D. H. Salesin. "Rendering parametric surfaces in pen and ink", Proc. SIGGRAPH 96, pp.469–476, 1996.

[49] S. Xu, C.M. Lau, F. Tang, Y. Pan, "Advanced Design for a Realistic Virtual Brush", Computer Graphics Forum, Vol. 22, Issue 3, 2003, pp. 533-542.

[50] S. Xu, M. Tang, F.C.M. Lau, and Y. Pan, "A Solid Model Based Virtual Hairy Brush", Computer Graphics Forum, Vol. 21, Issue 3, September 2002, pp. 299-308.

[51] Q. Zhang, Y. Sato, J. Takahashi, K. Muraoka and N. Chiba. "Simple cellular automaton-based simulation of ink behaviour and its application to suibokuga-like 3D rendering of trees", The Journal of Visualization and Computer Animation. Vol. 10, pp. 27-37, 1999.

[52] 3DEM Software http://www.visualizationsoftware.com.

[53] Stuart Green," Introduction to Non-Photorealistic Rendering", SIGGRAPH 99 Course 17, pp. 2.1 – 2.7.

Appendix 中英文專有名辭對照表

英文	中文
Axe-Cut Stroke	斧劈皴
Bean Strokes	豆瓣皴
Boneless Stroke	沒骨皴
Brush	筆
Ching Dynasty	清朝
Four Masters of the Yuan dynasty	元四大家
Four Treasures	文房四寶
Hemp-Fiber Stroke	批麻皴
Huang Kung-wang	黃公望
Hsia Kuei	夏珪
Ink Diffusion	水墨渲染
Ink Painting	水墨畫
Ink Stick	墨
Ink Stone	硯台
Ink Tone	墨色濃淡
Landscape Painting	山水畫
Li Tang	李唐
Lotus-Leaf Stroke	荷葉皴
Ma Yuan	馬遠
Mi-Dot Stroke	米點皴
Mi Fu	米芾
Outline	輪廓
Ox-hair Strokes	牛毛皴
Raindrop Stroke	雨點皴
Rice Paper	宣紙
Slanted Brush	側鋒
Splashed Ink Painting	潑墨畫
Sung Dynasty	宋朝
Tang Dynasty	唐朝
Texture Strokes	皴法
The Mustard Seed Garden	芥子園畫譜
Ts'un	皴法
Vertical Brush	中鋒

VITA

Der-Lor Way was born on February, 1963, in Keelung, Taiwan, Republic of China. He likes the drawing since childhood. He received the BS degree in computer science from Soochow University in 1986, MS degree in computer science from Chung-Yuan Christian University in 1988. He stayed in Communications and Computer Laboratory (CCL) to research multimedia and virtual reality for 11 years. He diligently is pursuing to integrate individual interest and his work. He found a new research field, non-photorealistic rendering, at SIGGRAPH conference in 1998. After one year, he decided to study a Ph.D. degree about Chinese ink painting in non-photorealistic rendering. He is currently a teacher in the Taipei National University of Arts. His research interests are in the area of non-photorealistic rendering and virtual reality.